D-wave quarkonium levels of the Υ family

Waikwok Kwong and Jonathan L. Rosner
Enrico Fermi Institute and Department of Physics, University of Chicago, Chicago, Illinois 60637
(Received 12 February 1988)

A key test of the nonrelativistic potential description of quarkonium is the confirmation of predicted D-wave levels. For the $b\bar{b}$ system (Υ family), the lowest spin-triplet levels ($1\,^3D$) are expected to lie in the range $10\,157\pm10$ MeV/c^2 and the next set of levels is expected in the range $10\,441\pm10$ MeV/c^2. Predictions are made for electric dipole transitions involving these levels, and specific suggestions are made for their observation. The most favorable decay chain appears to be $\Upsilon(3S)\to\gamma_1+2P\to\gamma_1+\gamma_2+1D\to\gamma_1+\gamma_2+\gamma_3+1P$, where γ_1 and γ_2 have energies of about 100 MeV and $E_{\gamma_3}\approx250$ MeV. Angular distributions of these photons are discussed.

I. INTRODUCTION

The study of heavy-quark bound states ("quarkonium") has led to a satisfactory picture of interquark force.[1] A central potential $V(r)$ appears to interpolate between short-distance Coulombic and long-distance linear behavior. For $0.1\le r\le1$ fm, $V(r)$ may be deduced largely on the basis of information about S-wave levels.[2] Solutions of the Schrödinger equation for this potential have led to accurate predictions of P-wave levels and (for systems of sufficiently heavy quarks, where relativistic effects are negligible) of electric-dipole transition rates. The main features of the interquark potential are understood on the basis of quantum chromodynamics (QCD), the gauge theory of the strong interactions.

It is of some interest to confirm further predictions of the potential description of quarkonium systems. It has been suggested, for example, that degrees of freedom associated with the quanta of the strong interactions, the *gluons*, prevent the potential from being a useful concept in hadron physics.[3]

The typical momentum of a quark in a hadron appears, via the uncertainty principle, to be several hundred MeV/c. The charmed quark, with a mass of about 1.5 GeV/c^2, can be treated crudely by nonrelativistic means. However, the lowest-mass systems for which a quantitative nonrelativistic approach can be expected to hold are the bound states of the b quark ($m_b\approx5$ GeV/c^2) and its antiquark.

The $b\bar{b}$ systems which have been discovered so far include a series of spin-triplet S-wave levels (at least six), and two spin triplets of P-wave levels. No D-wave states have been observed yet. The purpose of the present work is to predict the properties of the D-wave $b\bar{b}$ levels in as model-independent a manner as possible, and to make suggestions for their observation. We are guided in this effort by the existence of experiments which may be able to see such levels in the near future, particularly in e^+e^- annihilations[4] but also in hadronic production.[5]

Since the predicted D-wave levels are quite narrow, knowledge of their masses can also prevent hasty conclusions about the discovery of new fundamental particles such as Higgs bosons.

Our approach will be to use existing information on $b\bar{b}$ levels to construct an interquark potential via inverse-scattering methods.[6–11] We then use this potential to predict the masses of D-wave levels and to calculate bound-state wave functions. These, in turn, may be used to evaluate electric dipole transition matrix elements involving the predicted levels. A summary of predicted branching ratios for known and hypothetical states may be constructed, and suggestions made for observing the D-wave levels.

We conclude that the best hope for observing D-wave Υ levels lies in observing the three-photon cascade processes

$$\Upsilon(3S)\to\gamma_1(86-124\text{ MeV})+\chi_b'(2P)\,, \tag{1.1a}$$

$$\chi_b'(2P)\to\gamma_2(80-120\text{ MeV})+\Upsilon(1D)\,, \tag{1.1b}$$

$$\Upsilon(1D)\to\gamma_3(240-280\text{ MeV})+\chi_b(1P)\,. \tag{1.1c}$$

A useful "calibration" is provided by the processes

$$\Upsilon(3S)\to\gamma_1(86-124\text{ MeV})+\chi_b'(2P)\,, \tag{1.2a}$$

$$\chi_b'(2P)\to\gamma_2(205-242\text{ MeV})+\Upsilon(2S)\,, \tag{1.2b}$$

$$\Upsilon(2S)\to\gamma_3(110-160\text{ MeV})+\chi_b(1P)\,. \tag{1.2c}$$

For the cascades (1.2), all the photon energies and branching ratios are known. Another promising strategy is to observe four-photon cascades $3S\to2P\to1D\to1P\to1S$, followed by $1S\to e^+e^-$ or $\mu^+\mu^-$. The corresponding "calibration" involves replacement of $1D$ by $2S$ in this chain.

This paper is organized as follows. In Sec. II we review the inverse scattering method, and compare the predicted $b\bar{b}$ spectrum with that obtained in other approaches. Section III is devoted to calculation of electric dipole transition rates and to a summary of predicted decay rates and branching ratios for all spin-triplet $b\bar{b}$ levels of present interest. Experimental signatures for the D-wave levels, including angular distributions of photons in e^+e^- annihilations and some brief comments about $c\bar{c}$ $1D$ levels, are discussed in Sec. IV. We conclude in Sec. V. An Appendix contains details regarding photon angular distributions.

II. THE Υ SPECTRUM

Bound-state information is capable of reproducing a potential in the range of distances where the bound-state wave functions have appreciable values, via the inverse-scattering method. Simple examples from quantum mechanics have been given.[12,13] It has been possible to construct the interquark potential on the basis of $c\bar{c}$ data; the potential has then been used to predict satisfactorily the properties of the Υ levels (the $b\bar{b}$ bound states).[6,7] Using both $c\bar{c}$ and $b\bar{b}$ data on $^3S_1$ bound states, one can predict the positions of P-wave levels and the electric dipole transition rates between S- and P-wave levels.[8] These predictions, again, are borne out by experiment.

In this section we use inverse-scattering techniques to construct the $b\bar{b}$ potential, and then solve the Schrödinger equation for the D-wave levels. We shall use a simple model[14] for the fine structure of these levels.

A. Review of the inverse-scattering method

We shall recapitulate briefly the way in which energy levels and values of $|\Psi(0)|^2$ for S-wave quarkonium levels can allow the construction of an interquark potential which reproduces the physics of the P-wave levels and is thus expected to be a reliable source of D-wave predictions.

We begin with a simpler problem: Given N energy levels $E_1,\ldots,E_N$, construct a symmetric potential $V(x)=V(-x)$ tending to a value $E_0>(E_1,\ldots,E_N)$ at $x=\pm\infty$ and having just these levels. We use a technique which dates back to Darboux,[15] but which has been motivated most recently by appeal to supersymmetry,[16] to add levels one by one to a potential. This method is described in Ref. 11, and we do not reproduce it here.

Now, one really desires a central potential $V(r)$ useful for the three-dimensional Schrödinger equation. The reduced radial wave functions $u_n(r)=rR_n(r)$ for S-wave states obey the one-dimensional Schrödinger equation ($\hbar=1$)

$$\left[-\frac{1}{2\mu}\frac{d^2}{dr^2}+V(r)\right]u_n(r)=E_n u_n(r)\ , \tag{2.1}$$

where $\mu=m_Q/2$ is the reduced mass, and m_Q is the quark mass. The levels in (2.1) may be regarded as the odd-parity levels $u_n(r)=\psi_{2n}(r)$ in a symmetric potential $V(-r)=V(r)$, since $u_n(r)\sim r$ as $r\to 0$.

A one-dimensional symmetric potential $\tilde{V}(x)=\tilde{V}(-x)$ which has known values of E_{2n} and $\psi'_{2n}(0)$ can also be constructed via the inverse-scattering method. The values of $\psi'_{2n}(0)=u'_n(0)$ are provided by leptonic widths of $n\ ^3S_1$ bound quarkonium states:

$$\Gamma(nS\to e^+e^-)=\frac{4\alpha^2e_Q^2}{[M(nS)]^2}|u'_n(0)|^2a^{-1}\ , \tag{2.2}$$

where

$$a^{-1}=1-\frac{16\alpha_s}{3\pi} \tag{2.3}$$

is a QCD correction. The zeros of the function

$$f(E)=1+\sum_{k=1}^{N}\frac{|u'_k(0)|^2}{\kappa_k(E-E_k)}\ , \tag{2.4}$$

with

$$\kappa_k\equiv 2\mu(E_0-E_k) \tag{2.5}$$

are then the (unphysical) even-parity energy eigenvalues E_{2n-1} in the potential $\tilde{V}(x)$. Thus, one uses masses and leptonic widths of the lowest $N\ ^3S_1$ quarkonium levels to provide a set of values $E_1,\ldots,E_{2N}$ suitable for constructing an interquark potential. The quantity E_0, as mentioned, is the asymptotic value of $\tilde{V}(x)$ at $x=\pm\infty$:

$$\lim_{x\to\pm\infty}\tilde{V}(x)=E_0\ . \tag{2.6}$$

Smooth potentials $V(r)$ appear to be reproduced by the approximation $\tilde{V}(x)$ when E_0-E_{2N} is about half the level spacing at E_{2N}:[12]

$$E_0-E_{2N}\simeq(E_{2N}-E_{2N-1})/2\ . \tag{2.7}$$

B. Construction of an approximate $b\bar{b}$ potential

In Table I we summarize the Υ data used to construct a $b\bar{b}$ potential via the inverse-scattering method.[17] Small changes in the data[18] since this construction was performed have negligible effect.

The parameter a in Eq. (2.2) is expected to be approximately $[1-16\alpha_s(m_b)/3\pi]^{-1}\simeq 1.44$ for $\alpha_s(m_b)\simeq 0.18$, a value found in the analysis of quarkonium decays.[4,19] However, we leave a and E_0 as free parameters, adjusting them to obtain the most accurate predictions of $1P$ and $2P$ centers of gravity. These values are also shown in Table I. Again, recent small changes to these values do not affect the results.[18]

We then solve the Schrödinger equation for P-wave and D-wave $b\bar{b}$ levels in the potential constructed from the S-wave levels. Two different sets of results are shown in Table II, for the b-quark mass $m_b=4.5$ GeV/c with $a=1.3$ and for $m_b=4.9$ GeV/c^2 with $a=1.5$. The predictions are nearly indistinguishable from one another.

TABLE I. Parameters of Υ levels used to construct an interquark potential. nS and $1P$ masses from Ref. 17; $2P$ masses from Ref. 1.

Level	Mass (GeV/c^2)	Γ_{ee} (keV)
$\Upsilon(1S)$	9.4600(2)	1.224(50)
$\Upsilon(2S)$	10.0234(4)	0.537(33)
$\Upsilon(3S)$	10.3555(5)	0.402(31)
$\Upsilon(4S)$	10.5775(40)	0.240(45)
$\chi_b(1\ ^3P_0)$	9.8598(13)	
$\chi_b(1\ ^3P_1)$	9.8919(7)	$\langle 1P\rangle=9.9002$
$\chi_b(1\ ^3P_2)$	9.9133(6)	
$\chi_b(2\ ^3P_0)$	10.2305(23)	
$\chi_b(2\ ^3P_1)$	10.2557(8)	$\langle 2P\rangle=10.2601$
$\chi_b(2\ ^3P_2)$	10.2686(7)	

TABLE II. P-wave and D-wave centers of gravity in potential constructed from S-wave level parameters. All masses are in GeV/c^2, and $E_0=10.63$ GeV.

m_b (GeV/c^2)	4.5	4.9
a	1.3	1.5
$1P$	9.9026	9.9031
$2P$	10.2584	10.2589
$3P$	10.5197	10.5201
$1D$	10.1562	10.1567
$2D$	10.4408	10.4412

In accord with other discussions of potential models (see, e.g., Refs. 20–23) we choose the set of parameters based on $m_b=4.9$ GeV/c^2, $a=1.5$. The resulting potential may be found in Fig. 11 of Ref. 1.

C. Fine structure of D-wave levels

The general expression for terms contributing to fine structure in $Q\bar{Q}$ systems is

$$V_{\rm FS}(r)=V_{LS}(r)+V_{\rm tensor}(r)\ , \tag{2.8}$$

where

$$V_{LS}(r)=(\mathbf{L}\cdot\mathbf{S})[3\,dV_V(r)/dr-dV_S/dr]/(2m_Q^2 r)\ , \tag{2.9}$$

$$V_{\rm tensor}(r)=(S_{12}/12m_Q^2)(r^{-1}dV_V/dr-d^2V_V/dr^2)\ , \tag{2.10}$$

and

$$S_{12}\equiv 2[3(\mathbf{S}\cdot\hat{\mathbf{r}})(\mathbf{S}\cdot\hat{\mathbf{r}})-\mathbf{S}^2]\ . \tag{2.11}$$

Here V_V and V_S denote potentials associated with vector and scalar exchange, respectively. A convenient expression for $\langle S_{12}\rangle$ (see, e.g., Ref. 24) is

$$\langle S_{12}\rangle=-[(2l-1)(2l+3)]^{-1}(12\langle\mathbf{L}\cdot\mathbf{S}\rangle^2+6\langle\mathbf{L}\cdot\mathbf{S}\rangle-4\langle\mathbf{S}^2\rangle\langle\mathbf{L}^2\rangle)\ . \tag{2.12}$$

where $\langle\mathbf{L}^2\rangle=l(l+1)$. The matrix elements of $\mathbf{L}\cdot\mathbf{S}$ and S_{12} for P, D, and F states are summarized in Table III.

The fine structure of the P-wave $b\bar{b}$ levels suggests[1,4,14,23] that the short-range (Coulombic) part of the potential behaves as vector exchange, while the long-range (linear) part behaves as a scalar. There is some theoretical support for this picture,[14,25] though opinion is not unanimous,[15,26,27] and we shall adopt it for present purposes.

We thus take

$$V_V(r)=-\frac{4}{3}\frac{\alpha_s}{r}\ , \tag{2.13}$$

$$V_S(r)=kr\ , \tag{2.14}$$

so that

TABLE III. Matrix elements of angular momentum operators for ^3P, ^3D, and ^3F states of quarkonium.

	$\langle\mathbf{L}\cdot\mathbf{S}\rangle$	$\langle S_{12}\rangle$
$^3P_0$	−2	−4
$^3P_1$	−1	2
$^3P_2$	1	$-\frac{2}{5}$
$^3D_1$	−3	−2
$^3D_2$	−1	2
$^3D_3$	2	$-\frac{4}{7}$
$^3F_2$	−4	$-\frac{8}{5}$
$^3F_3$	−1	2
$^3F_4$	3	$-\frac{2}{3}$

$$M(^3L_J)=\bar{M}(^3L)+a\langle\mathbf{L}\cdot\mathbf{S}\rangle+b\langle S_{12}\rangle\ , \tag{2.15}$$

with

$$a=(4\alpha_s\langle r^{-3}\rangle-k\langle r^{-1}\rangle)/2m_Q^2\ , \tag{2.16}$$

$$b=\alpha_s\langle r^{-3}\rangle/3m_Q^2\ . \tag{2.17}$$

The values of $\langle r^{-1}\rangle$ and $\langle r^{-3}\rangle$ were evaluated for states in the potential described earlier, with results summarized in Table IV.

The values of a and b for the $1\,^3P_J$ and $2\,^3P_J$ levels can be obtained from their masses M_J:

$$a=(-2M_0-3M_1+5M_2)/12\ , \tag{2.18}$$

$$b=5(-2M_0+3M_1-M_2)/72\ . \tag{2.19}$$

These values are shown in italics in Table IV. They may be used to determine the independent parameters α_s/m_b^2 and $k/2m_b^2$ in Eqs. (2.16) and (2.17). An average of determinations from the $1P$ and $2P$ levels yields

$$\alpha_s/m_b^2=0.016\ \text{GeV}^{-2}\ , \tag{2.20}$$

$$k/2m_b^2=0.0049\ . \tag{2.21}$$

With the help of the values of $\langle r^{-1}\rangle$ and $\langle r^{-3}\rangle$ quoted in Table IV, these then yield values of a and b, also quoted there.

TABLE IV. Parameters governing fine structure in $b\bar{b}$ levels. Values of a and b in italics are obtained from observed masses.

Level	$\langle r^{-1}\rangle$ (GeV)	$\langle r^{-3}\rangle$ (GeV^3)	a (MeV)	b (MeV)
$1P$	0.635	0.550	*14.27*	*2.97*
$2P$	0.445	0.394	*10.35*	*2.04*
$3P$	0.316	0.261	6.90	1.41
$1D$	0.430	0.120	1.78	0.65
$2D$	0.340	0.105	1.71	0.56
$1F$	0.333	0.049	−0.06	0.26

The value of $\alpha_s=0.39$ and $k=0.24$ GeV^2 implied by Eqs. (2.20) and (2.21) (for $m_b=4.9$ GeV/c^2) are rather large, suggesting that the present model may have mainly phenomenological rather than fundamental significance. A large effective value of α_s was also found in Ref. 14.

Our results for the masses of ^3D states are compared with those of other authors[21,22,27] in Table V. The fine structure is predicted to be somewhat smaller in the present model than that of other authors, but there is a general agreement on masses to within ± 10 MeV. The predicted level structure of $3P$, $1D$, and $2D$ states is placed in the context of observed S- and P-wave levels in Fig. 1.

We also expect a triplet of $1F$ levels, with negligible fine structure, at a mass of 10.348 GeV/c^2. Neither these levels nor the spin-singlet $b\bar{b}$ levels are shown in Fig. 1. The level structure in Fig. 1 is remarkably close to that anticipated by Sterling,[28] just after the discovery of the Υ levels, on the basis of a logarithmic potential. In fact, for $V(r)=(0.72\text{ GeV})\ln r+\text{const}$, one expects

$$M(1S,2S,3S,4S)$$
$$=(9.46[\text{input}],10.04,10.36,10.58)\text{ GeV}/c^2\ ;$$
$$M(1P,2P,3P)=(9.89,10.26,10.50)\text{ GeV}/c^2\ ;$$
$$M(1D,2D)=(10.16,10.43)\text{ GeV}/c^2\ ;$$
$$M(1F)=10.35\text{ GeV}/c^2\ .$$

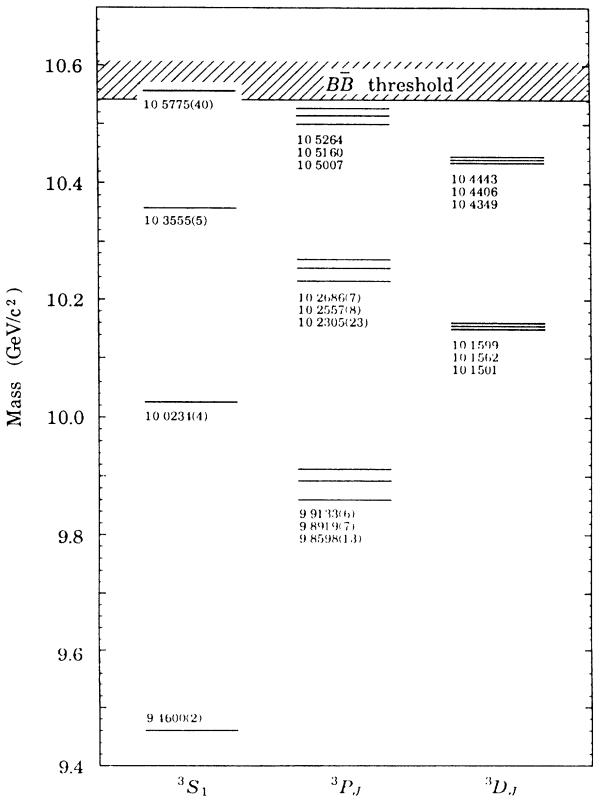

FIG. 1. Masses of S-, P-, and D-wave $b\bar{b}$ levels, in GeV/c^2. Numbers in parentheses correspond to experimental errors in last digit(s), for observed states.

TABLE V. Comparison of predictions for masses of $\Upsilon(1D)$ and $\Upsilon(2D)$ levels, in GeV/c^2.

	Ref. 21	Ref. 22	Ref. 27	This work
$1\,^3D_1$	10.151	10.155	10.153	10.150
$1\,^3D_2$	10.161	10.162	10.163	10.156
$1\,^3D_3$	10.168	10.167	10.174	10.160
$\langle 1D\rangle$	10.162	10.163	10.166	10.157
$2\,^3D_1$	10.433	10.447	10.444	10.435
$2\,^3D_2$	10.441	10.454	10.452	10.441
$1\,^3D_3$	10.447	10.459	10.462	10.444
$\langle 2D\rangle$	10.442	10.455	10.455	10.441

III. TRANSITION RATES

A. Electric dipole transitions

The transition rate between an initial quarkonium state i of radial quantum number n_i, orbital angular momentum L_i, spin S_i, and total angular momentum J_i, and a final state f with corresponding labels is given by ($\hbar=c=1$; $S_i=S_f\equiv S$) (Refs. 20, 21, and 28)

$$\Gamma(n_iL_iS_iJ_i\to n_fL_fS_fJ_f)$$
$$=\tfrac{4}{3}e_Q^2\alpha\omega^3C(J_iL_iJ_fL_fS)\delta_{S_iS_f}\langle r\rangle^2\ , \quad (3.1)$$

where e_Q is the quark charge in units of $|e|$, ω is the photon energy,

$$C(J_iL_iJ_fL_fS)=\max(L_i,L_f)(2J_f+1)\begin{Bmatrix}L_f & J_f & S\\ J_i & L_i & 1\end{Bmatrix}^2\ . \quad (3.2)$$

and

$$\langle r\rangle\equiv\int_0^\infty rR_{n_fL_f}(r)R_{n_iL_i}(r)r^2dr\ . \quad (3.3)$$

Here the radial wave functions are normalized in such a way that

$$\int_0^\infty R_{nL}(r)R_{n'L}(r)r^2dr=\delta_{nn'}\ . \quad (3.4)$$

The coefficients (3.2) for cases of interest to us are summarized in Table VI. The values of the overlap integrals (3.3) are given in Table VII, along with photon energies and predicted rates. These are compared for $S\to P$ transitions with measured values quoted in Refs. 17 and 29. The agreement, including for the highly suppressed $3S\to 1P$ transitions, is satisfactory.

The dipole matrix elements in Table VII are very close to those found previously by other authors.[8,20–22,28] For example, they differ by less than a few percent (except for

TABLE VI. Summary of coefficients $C(J_i L_k J_f L_f S)$ entering into electric dipole transition rates (2.18).

$^3S_1 \to {}^3P_J$: $(2J_f+1)/9$

$^3P_J \to {}^3S_1$: $\frac{1}{3}$

$^3P_J \to {}^3D_{J'}$

J \ J'	1	2	3
0	$\frac{2}{3}$	0	0
1	$\frac{1}{6}$	$\frac{1}{2}$	0
2	$\frac{1}{150}$	$\frac{1}{10}$	$\frac{14}{25}$

$^3D_J \to {}^3P_{J'}$

J \ J'	0	1	2
1	$\frac{2}{9}$	$\frac{1}{6}$	$\frac{1}{90}$
2	0	$\frac{3}{10}$	$\frac{1}{10}$
3	0	0	$\frac{2}{5}$

the highly suppressed $3S \to 1P$ transition) from those obtained in Ref. 28. This is another illustration (cf. Ref. 2) that all potentials which reproduce previously observed S- and P-wave $b\bar{b}$ levels agree with one another in the relevant range of distance for calculating the matrix elements in question.

The total widths of $1P$ and $2P$ states are needed for a comparison of predicted $P \to S$ rates with experiment, since only branching ratios of $P \to S$ transitions, and not absolute rates, are measured. We calculate these total widths in Sec. III B.

B. Hadronic widths and summaries of branching ratios

1. P states.

The derivative of the radial wave function at the origin governs the amplitude for annihilation of a $^3P_{0,2}$ quarkonium state into gluons or a $^3P_1$ state into $q\bar{q}$ + glue. The relevant expressions, containing lowest-order QCD corrections, for $b\bar{b}$ states are[19]

$$\Gamma(^3P_0 \to \text{glue}) = \frac{6\alpha_s^2 |R'_{nP}(0)|^2}{m_b^4} \times \begin{cases} (1+10\alpha_s/\pi) & (1P), \\ (1+10.2\alpha_s/\pi) & (2P), \end{cases} \tag{3.5}$$

$$\Gamma(^3P_1 \to q\bar{q} + \text{glue}) = \frac{32}{9\pi} \frac{\alpha_s^3 |R'_{nP}(0)|^2}{m_b^4} \ln(m_b \langle r \rangle), \tag{3.6}$$

$$\Gamma(^3P_2 \to \text{glue}) = \frac{8\alpha_s^2 |R'_{nP}(0)|^2}{5m_b^4} \times \begin{cases} (1-0.1\alpha_s/\pi) & (1P), \\ (1+1.0\alpha_s/\pi) & (2P). \end{cases} \tag{3.7}$$

In Eq. (3.6) we have assumed four flavors of light quarks. The values of $|R'_{nP}(0)|^2$ are found by calculation to be (1.416, 1.538, 1.233) GeV^5, while $\langle r \rangle = (1.86, 3.05, 4.53)$ GeV^{-1}, for $(1P, 2P, 3P)$ states.

In Table VIII we summarize predicted partial and total widths of the $1P$ and $2P$ levels, thereby predicting branching ratios for $P \to S$ radiative transitions. These are compared with experimental values from Refs. 17 ($1P \to 1S$) and 4 ($2P \to 1S, 2S$). Apart from the transition $2\,^3P_1 \to \gamma + 1\,^3S_1$, for which the rate quoted in Ref. 4 seems anomalously low, every prediction agrees with experiment to within two standard deviations. Relativistic corrections[21,30] are more likely to affect processes with hard photons such as the one just mentioned, but we do not expect them to be more than about 30% in rate.[21]

In a previous account of hadronic widths of the $1P$ and $2P$ levels,[1] we quoted total widths of (382, 64, 132) keV for the $J=(0,1,2)$ $1P$ states, and (336, 60, 116) keV for the $J=(0,1,2)$ $2P$ states. Those results were based upon (a) an older value of $\alpha_s = 0.158$, (b) neglect of QCD corrections, and (c) use of M(state)/2 rather than m_b in the formula for the decay rates corresponding to Eqs. (3.5)–(3.7), except that in the logarithm of Eq. (3.6) we used $M(\text{state})\langle r \rangle$. We regard the widths of Table VIII as superseding the previous values.

The transitions $2\,^3P_J \to 1\,^3P_J \pi\pi$ have been neglected in the above discussions. It has been estimated[31] that these occur with rates of 0.3–0.4 keV for each J, which would not significantly affect $2\,^3P_J$ total widths.

2. D states.

The hadronic transitions of ^3D states are of two types:

$$\Upsilon(D) \to 3 \text{ gluons} \tag{3.8}$$

and

$$\Upsilon(D) \to \pi\pi\Upsilon(S). \tag{3.9}$$

Estimates of both of these have appeared recently.[32,33]

The rates for $\Upsilon(D) \to 3$ gluons are dominated to leading order in logarithms by processes in which one of the three gluons is soft. (Two gluons cannot be emitted in ^3D decays since the charge-conjugation eigenvalue of a ^3D state is odd.) The resulting expressions for the decay widths[32] are

$$\Gamma(^3D_1 \to 3g) = \frac{760}{81\pi} \frac{\alpha_s^3 |R''_D(0)|^2}{m_b^6} \ln(4m_b \langle r \rangle), \tag{3.10}$$

$$\Gamma(^3D_2 \to 3g) = \frac{10}{9\pi} \frac{\alpha_s^3 |R''_D(0)|^2}{m_b^6} \ln(4m_b \langle r \rangle), \tag{3.11}$$

$$\Gamma(^3D_3 \to 3g) = \frac{40}{9\pi} \frac{\alpha_s^3 |R''_D(0)|^2}{m_b^6} \ln(4m_b \langle r \rangle). \tag{3.12}$$

For the $1D$ levels, Bélanger and Moxhay find $\Gamma(^3D_J \to 3g) = (2.2, 0.26, 1.1)$ keV for $J=(1,2,3)$.

The transitions (3.9) have been the subject of some question in the literature. Billoire, Lacaze, Morel, and Navelet[34] estimated $\Gamma(\Upsilon(1D) \to \Upsilon(1S)\pi\pi) = 0.07\alpha_s^2$ keV, while Kuang and Yan[31] predicted 24 keV, both results

TABLE VII. Dipole matrix elements $\langle r \rangle$ [Eq. (2.24)] for transitions in $b\bar{b}$ states, and corresponding predictions for rates [Eq. (2.22)]. Experimental numbers are taken from Ref. 17 unless noted otherwise.

(a) $S \to P$ transitions

Transition	$\langle r \rangle$ (GeV^{-1})	J_i	J_f	ω (MeV)	Γ (keV) Predicted	Γ (keV) Observed
$2S \to 1P$	-1.646	1	0	162.3±1.3	1.39	1.29±0.43[a]
			1	130.7±0.7	2.18	2.02±0.55[a]
			2	109.5±0.6	2.14	1.97±0.55[a]
$3S \to 1P$	0.023	1	0	483.8±1.4	0.007	
			1	453.2±0.9	0.017	0.041±0.029[b]
			2	432.8±0.8	0.025	0.064±0.045[b]
$3S \to 2P$	-2.672	1	0	124.2±2.3	1.65	1.4±0.7[b]
			1	99.3±0.8	2.52	3.0±1.0[b]
			2	86.5±0.7	2.78	3.3±1.1[b]

(b) $P \to S$ transitions

Transition	$\langle r \rangle$ (GeV^{-1})	J_f	J_i	ω (MeV)	Γ (keV) Predicted
$1P \to 1S$	1.098	1	0	391.7±1.3	26.1
			1	442.5±0.7	32.8
			2	442.9±0.6	37.8
$2P \to 1S$	0.240	1	0	741.5±2.3	8.48
			1	764.8±0.8	9.31
			2	776.8±0.7	9.75
$2P \to 2S$	1.911	1	0	205.0±2.3	11.3
			1	229.7±0.9	15.9
			2	242.3±0.8	18.7
$3P \to 1S$	0.101	1	0	989	3.54
			1	1003	3.69
			2	1012	3.80
$3P \to 2S$	0.298	1	0	466	3.24
			1	481	3.56
			2	491	3.78
$3P \to 3S$	2.627	1	0	144	7.46
			1	159	10.1
			2	170	12.1

(c) $P \to D$ transitions

Transition	$\langle r \rangle$ (GeV^{-1})	J_i	J_f	ω (MeV)	Γ (keV) Predicted
$2P \to 1D$	-1.877	0	1	81.2	1.36
		1	1	106.1	0.76
			2	99.2	1.86
		2	1	118.9	0.043
			2	112.0	0.54
			3	107.0	2.62
$3P \to 1D$	0.0023	All transitions negligible			
$3P \to 2D$	-3.015	0	1	66	1.85
		1	1	81	0.86
			2	75	2.08
		2	1	91	0.050
			2	85	0.61
			3	82	3.01

TABLE VII. (*Continued*).

(d) $D \rightarrow P,F$ transitions

Transition	$\langle r \rangle$ (GeV^{-1})	J_i	J_f	ω (MeV)	Γ (keV) Predicted
$1D \rightarrow 1P$	1.959	1	0	285	21.4
			1	254	11.3
			2	233	0.58
		2	1	261	22.0
			2	240	5.7
		3	2	245	24.3
$2D \rightarrow 1P$	0.256	1	0	559	2.76
			1	529	1.75
			2	509	0.10
		2	1	534	3.25
			2	514	0.97
		3	2	518	3.94
$2D \rightarrow 2P$	2.672	1	0	202	14.2
			1	178	7.2
			2	165	0.38
		2	1	183	14.2
			2	171	3.83
		3	2	174	16.3
$2D \rightarrow 1F$	−2.006	1	2	86.5	1.69
		2	2	92.2	0.23
			3	91.4	1.77
		3	2	95.9	0.005
			3	95.1	0.18
			4	96.0	2.12

[a]Based on total $\Upsilon(2S)$ width of 30.0±7.3 keV quoted in Ref. 17.
[b]Based on total $\Upsilon(3S)$ width of 25.5±5.0 keV quoted in Ref. 29. The $3S \rightarrow 1P$ transitions were reported in Ref. 4.

being independent of J. Very recently Moxhay[33] has found that the former number is essentially the correct one, obtaining

$$\Gamma(\Upsilon(1D) \rightarrow \Upsilon(1S)\pi\pi) = 0.07 \text{ keV} \tag{3.13}$$

for $^3D_{1,2,3}$ states.

The crucial point leading to the suppression of the $\Upsilon\pi\pi$ decays is as follows. The transition $\Upsilon(1D) \rightarrow \Upsilon(1S)\pi\pi$ proceeds in two steps. The quarks in the $1D$ states emit two gluons in an overall color singlet state, and end up in a $1S$ state. The two gluons then materialize into two pions. Now, the emission of gluons takes place without change of quark spin, to lowest order in gluon momenta. The transition then may be regarded as one proceeding from $L=2$ to $L=0$ states of spinless quarks. Thus the gluons must carry off two units of angular momenta: $L_{\text{gluons}}=2$.

Call $L_{\pi\pi}$ the orbital angular momenta of the two pions in their rest frame ($L_{\pi\pi}$ is even since $I_{\pi\pi}=0$), and $L_{\pi\pi,\Upsilon}$ the orbital angular momentum of the two-pion system with respect to the Υ. We have

$$\mathbf{L}_{\pi\pi} + \mathbf{L}_{\pi\pi,\Upsilon} = \mathbf{L}_{\text{gluons}} , \tag{3.14}$$

and $L_{\text{gluons}}=2$. In either case one cannot avoid substantial centrifugal barriers. Billoire, Lacaze, Morel, and Navelet[34] encountered such barriers when projecting into the state $L_{\pi\pi}=0$, but they must clearly be present in all cases. Kuang and Yan did not project the two gluons emitted in $\Upsilon(1D) \rightarrow \Upsilon(1S)+2g$ into any final state, and so did not encounter the barrier suppression.

In Table IX we summarize the expected $1D$ branching ratios. Electromagnetic decays to $1P$ levels are dominant. The small e^+e^- width of the $1\,^3D_1$ level, 1.5 eV, was calculated in Ref. 21. A similar table may be prepared for the $2D$ levels once their $3g$ and $\Upsilon\pi\pi$ widths have been calculated. One expects these widths to be small, however, and so the electromagnetic transitions listed in Table VII(d) will be the dominant decays of the $2D$ levels. In Ref. 21 the value $\Gamma(2\,^3D_1 \rightarrow e^+e^-)=2.7$ eV was found.

Qualitatively similar branching ratios to those quoted

TABLE VIII. Predicted partial and total widths of $1\,^3P_J$ and $2\,^3P_J$ $b\bar{b}$ levels, and predicted branching ratios (B). Also shown are measured branching ratios for $1P \to 1S$ radiative transitions (Ref. 17) and $2P \to (1S, 2S)$ transitions (Ref. 4).

Level	Final state	Predicted Width (keV)	Predicted B (%)	Measured B (%)
$1\,^3P_0$	glue	791	96.8	
	$\gamma+1S$	26.1	3.2	<6
	all	817	100	
$1\,^3P_1$	$q\bar{q}+$glue	38.3	53.9	
	$\gamma+1S$	32.8	46.1	35±8
	all	71.1	100	
$1\,^3P_2$	glue	132.3	77.8	
	$\gamma+1S$	37.8	22.2	22±4
	all	170.1	100	
$2\,^3P_0$	glue	866	97.6	
	$\gamma+1S$	8.48	0.96	1.4±1.0
	$\gamma+2S$	11.3	1.27	6.9±3.8
	$\gamma+1\,^3D_1$	1.36	0.153	
	all	887	100	
$2\,^3P_1$	glue	50.9	64.7	
	$\gamma+1S$	9.31	11.8	6.1±1.3
	$\gamma+2S$	15.9	20.2	24.7±6.9
	$\gamma+1\,^3D_1$	0.76	0.97	
	$\gamma+1\,^3D_2$	1.86	2.36	
	all	78.7	100	
$2\,^3P_2$	glue	153.0	82.9	
	$\gamma+1S$	9.75	5.3	6.3±1.3
	$\gamma+2S$	18.7	10.1	18.9±5.3
	$\gamma+1\,^3D_1$	0.043	0.023	
	$\gamma+1\,^3D_2$	0.54	0.29	
	$\gamma+1\,^3D_3$	2.62	1.42	
	all	184.7	100	

TABLE IX. Summary of predicted partial widths and branching ratios (B) for $1D$ $b\bar{b}$ levels.

Level	Final state	Predicted Width (keV)	Predicted B (%)
$1\,^3D_1$	$\gamma+1\,^3P_0$	21.4	60.2
	$\gamma+1\,^3P_1$	11.3	31.8
	$\gamma+1\,^3P_2$	0.58	1.6
	$3g$	2.2	6.2
	$\Upsilon\pi\pi$	0.07	0.2
	e^+e^-	0.0015	0.0042
	all	35.6	100
$1\,^3D_2$	$\gamma+1\,^3P_0$	22.0	78.5
	$\gamma+1\,^3P_2$	5.7	20.3
	$3g$	0.26	0.9
	$\Upsilon\pi\pi$	0.07	0.2
	all	28.0	100
$1\,^3D_3$	$\gamma+1\,^3P_2$	24.3	95.4
	$3g$	1.1	4.3
	$\Upsilon\pi\pi$	0.07	0.3
	all	25.5	100

in Tables VII–IX appear in the early compendium of Ref. 28.

The smallness of the expected $\Upsilon\pi\pi$ decays of D-wave $b\bar{b}$ levels means that one will have to rely primarily on multiphoton cascades to discover the D waves. We discuss in Sec. IV ways of utilizing this information.

IV. EXPERIMENTAL SIGNATURES

A. Electromagnetic transitions from the Υ(3S)

We summarize the number of inclusive photons coming from 10^6 $\Upsilon(3S)$ decays, on the basis of our *predicted* branching ratios for transitions. These are sorted via transition in Table X(a) and via photon energy in Table X(b). We have ignored any transitions involving spin-singlet states. Photons from transitions involving the D states are expected to be present at a level of at most a few percent of the dominant $3S\rightarrow 2P$ photons, and tens of percent of the abundant $2P\rightarrow 2S$ photons. In Fig. 2 we show an inclusive photon spectrum calculated from Table X(b) with a Gaussian resolution function with[4] $\sigma_E/E=2.0\%\ [E(\mathrm{GeV})]^{1/4}$. It is unlikely that any photons involving $P\rightarrow D$ or $D\rightarrow P$ transitions will be visible in inclusive spectra. We turn next to methods which may hold some promise for revealing the D states.

1. Three-photon cascades

In Fig. 3 we compare two three-photon cascade processes starting from the $\Upsilon(3S)$. The first, Fig. 3(a), $3S\rightarrow 2P\rightarrow 2S\rightarrow 1P$, involves known branching ratios and photon energies. Normally the cascades $3S\rightarrow 2P\rightarrow 2S$ are identified via the subsequent e^+e^- or $\mu^+\mu^-$ decay of the $2S$. However, if the three-photon cascades in Fig. 3(a) can be observed, there is hope for observing the corresponding $3S\rightarrow 2P\rightarrow 1D\rightarrow 1P$ cascades shown in Fig. 3(b). The two cascades are to be distinguished from one another on the basis of the energies of γ_2 and γ_3. With present expectations for the masses of the $1D$ levels, this turns out to be possible with present resolution.

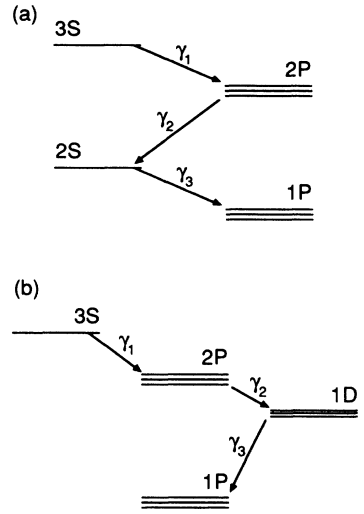

FIG. 3. Schematic diagrams of three-photon cascades from $\Upsilon(3S)$ to $1P$ levels. (a) $3S\rightarrow 2P\rightarrow 2S\rightarrow 1P$; (b) $3S\rightarrow 2P\rightarrow 1D\rightarrow 1P$.

The specific transitions to different members of the fine-structure multiplets are summarized in Fig. 4. In Table XI we list the photon energies for three-photon cascades from the $3S$ to the $1P$ levels, and summarize the combined branching ratios B in Table XII. The most

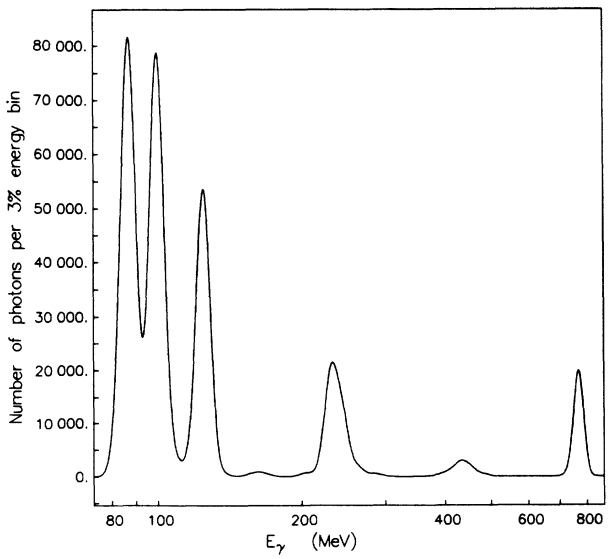

FIG. 2. Inclusive photon spectra expected from 10^6 $\Upsilon(3S)$, smeared with a Gaussian resolution function of the form $\sigma_E/E=2.0\%[E\ (\mathrm{GeV})]^{1/4}$.

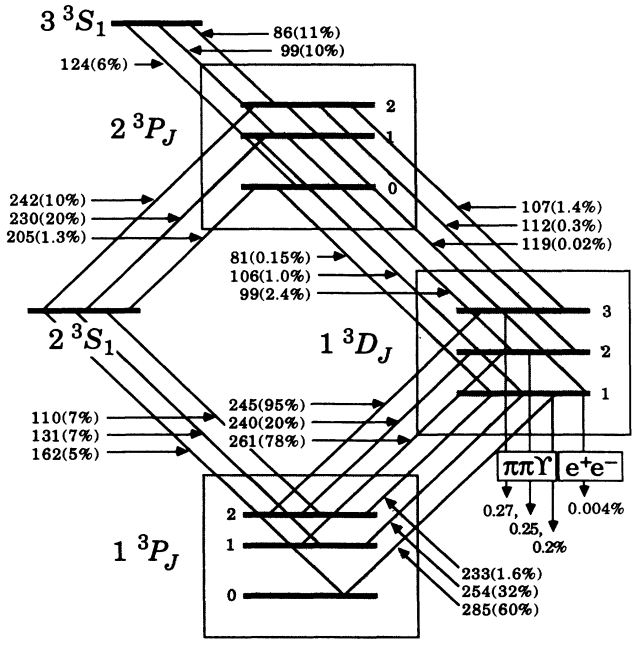

FIG. 4. Branching ratios for radiative transitions in three-photon cascades from $\Upsilon(3\,^3S_1)$ to $\chi_b(1\,^3P_J)$ levels.

TABLE X. (a) Inclusive photon spectra from upsilon (3S). Only electric dipole transitions considered. (b) Inclusive photon spectra from upsilon (3S), sorted via photon energies. (Electric dipole transitions only.)

Transition	Energy (MeV)	B (%)	Relative abundance (per million of 3S)	Doppler broadening (%)	Doppler broadening (MeV)
			(a)		
$3\,^3S_1 \to 2\,^3P_2$	86.54	10.90	109 000	0.00	0.00
$3\,^3S_1 \to 2\,^3P_1$	99.32	9.89	98 900	0.00	0.00
$3\,^3S_1 \to 2\,^3P_0$	124.25	6.45	64 500	0.00	0.00
$3\,^3S_1 \to 1\,^3P_2$	432.76	0.10	970	0.00	0.00
$3\,^3S_1 \to 1\,^3P_1$	453.22	0.07	670	0.00	0.00
$3\,^3S_1 \to 1\,^3P_0$	483.84	0.03	270	0.00	0.00
$2\,^3S_1 \to 1\,^3P_2$	109.50	7.12	2 270	3.30	3.61
$2\,^3S_1 \to 1\,^3P_1$	130.64	7.26	2 315	3.30	4.31
$2\,^3S_1 \to 1\,^3P_0$	162.26	4.64	1 479	3.30	5.35
$2\,^3P_2 \to 2\,^3S_1$	242.27	10.13	11 042	0.82	1.99
$2\,^3P_2 \to 1\,^3S_1$	776.76	5.28	5 755	0.82	6.37
$2\,^3P_2 \to 1\,^3D_3$	107.04	1.42	1 548	0.82	0.88
$2\,^3P_2 \to 1\,^3D_2$	111.98	0.29	316	0.82	0.92
$2\,^3P_2 \to 1\,^3D_1$	118.90	0.02	25	0.82	0.97
$2\,^3P_1 \to 2\,^3S_1$	229.67	20.24	20 017	0.98	2.25
$2\,^3P_1 \to 1\,^3S_1$	764.83	11.82	11 690	0.98	7.50
$2\,^3P_1 \to 1\,^3D_2$	99.22	2.36	2 334	0.98	0.97
$2\,^3P_1 \to 1\,^3D_1$	106.14	0.96	949	0.98	1.04
$2\,^3P_0 \to 2\,^3S_1$	205.00	1.28	826	1.20	2.46
$2\,^3P_0 \to 1\,^3S_1$	741.49	0.96	619	1.20	8.90
$2\,^3P_0 \to 1\,^3D_1$	81.18	0.15	99	1.20	0.97
$1\,^3D_3 \to 1\,^3P_2$	244.68	95.41	1 477	1.91	4.67
$1\,^3D_2 \to 1\,^3P_2$	239.80	20.36	540	1.96	4.70
$1\,^3D_2 \to 1\,^3P_1$	260.67	78.46	2 079	1.96	5.11
$1\,^3D_1 \to 1\,^3P_2$	232.96	1.64	18	2.03	4.73
$1\,^3D_1 \to 1\,^3P_1$	253.84	31.84	342	2.03	5.15
$1\,^3D_1 \to 1\,^3P_0$	285.08	60.13	645	2.03	5.79
$1\,^3P_2 \to 1\,^3S_1$	442.94	22.20	1 171	4.46	19.76
$1\,^3P_1 \to 1\,^3S_1$	442.47	46.11	2 493	4.69	19.81
$1\,^3P_0 \to 1\,^3S_1$	391.69	3.19	76	5.03	19.70
			(b)		
$2\,^3P_0 \to 1\,^3D_1$	81.18	0.15	99	1.20	0.97
$3\,^3S_1 \to 2\,^3P_2$	86.54	10.90	109 000	0.00	0.00
$2\,^3P_1 \to 1\,^3D_2$	99.22	2.36	2 334	0.98	0.97
$3\,^3S_1 \to 2\,^3P_1$	99.32	9.89	98 900	0.00	0.00
$2\,^3P_1 \to 1\,^3D_1$	106.14	0.96	949	0.98	1.04
$2\,^3P_2 \to 1\,^3D_3$	107.04	1.42	1 548	0.82	0.88
$2\,^3S_1 \to 1\,^3P_2$	109.50	7.12	2 270	3.30	3.61
$2\,^3P_2 \to 1\,^3D_2$	111.98	0.29	316	0.82	0.92
$2\,^3P_2 \to 1\,^3D_1$	118.90	0.02	25	0.82	0.97
$3\,^3S_1 \to 2\,^3P_0$	124.25	6.45	64 500	0.00	0.00
$2\,^3S_1 \to 1\,^3P_1$	130.64	7.26	2 315	3.30	4.31
$2\,^3S_1 \to 1\,^3P_0$	162.26	4.64	1 479	3.30	5.35
$2\,^3P_0 \to 2\,^3S_1$	205.00	1.28	826	1.20	2.46
$2\,^3P_1 \to 2\,^3S_1$	229.67	20.24	20 017	0.98	2.25
$1\,^3D_1 \to 1\,^3P_2$	232.96	1.64	18	2.03	4.73
$1\,^3D_2 \to 1\,^3P_2$	239.80	20.36	540	1.96	4.70
$2\,^3P_2 \to 2\,^3S_1$	242.27	10.13	11 042	0.82	1.99
$1\,^3D_3 \to 1\,^3P_2$	244.68	95.41	1 477	1.91	4.67
$1\,^3D_1 \to 1\,^3P_1$	253.84	13.84	342	2.03	5.15
$1\,^3D_2 \to 1\,^3P_1$	260.67	78.46	2 079	1.96	5.11
$1\,^3D_1 \to 1\,^3P_0$	285.08	60.13	645	2.03	5.79
$1\,^3P_0 \to 1\,^3S_1$	391.69	3.19	76	5.03	19.70
$1\,^3P_1 \to 1\,^3S_1$	422.47	46.11	2 493	4.69	19.81
$3\,^3S_1 \to 1\,^3P_2$	432.76	0.10	970	0.00	0.00
$1\,^3P_2 \to 1\,^3S_1$	442.94	22.20	1 171	4.46	19.76

TABLE X. (*Continued*).

Transition	Energy (MeV)	B (%)	Relative abundance (per million of $3S$)	Doppler broadening (%)	Doppler broadening (MeV)
$3\,^3S_1 \to 1\,^3P_1$	453.22	0.07	670	0.00	0.00
$3\,^3S_1 \to 1\,^3P_0$	483.84	0.03	270	0.00	0.00
$2\,^3P_0 \to 1\,^3S_1$	741.49	0.96	619	1.20	8.90
$2\,^3P_1 \to 1\,^3S_1$	764.83	11.82	11 690	0.98	7.50
$2\,^3P_2 \to 1\,^3S_1$	776.76	5.28	5 755	0.82	6.37

prominent cascades involving $1D$ states include

$$3S \to 2\,^3P_1 \to 1\,^3D_2 \to 1\,^3P_1 (B = 1.83 \times 10^{-3}) , \quad (4.1)$$

$$3S \to 2\,^3P_2 \to 1\,^3D_3 \to 1\,^3P_2 (B = 1.48 \times 10^{-3}) . \quad (4.2)$$

These are comparable in strength to three-photon cascades through the $2S$ level, the most prominent of which are

$$3S \to 2\,^3P_1 \to 2S \to 1\,^3P_1 (B = 1.45 \times 10^{-3}) , \quad (4.3)$$

$$3S \to 2\,^3P_1 \to 2S \to 1\,^3P_2 (B = 1.42 \times 10^{-3}) , \quad (4.4)$$

$$3S \to 2\,^3P_2 \to 2S \to 1\,^3P_1 (B = 0.80 \times 10^{-3}) , \quad (4.5)$$

$$3S \to 2\,^3P_2 \to 2S \to 1\,^3P_2 (B = 0.78 \times 10^{-3}) . \quad (4.6)$$

In order to see whether the cascades involving $1D$ states can be separated from those involving $2S$ states, we plot in Fig. 5 the number of events expected for specific energies of the second and third photon in the cascade, assuming that the energy of the first photon can be resolved well enough to select the transition $3S \to 2\,^3P_2$ [Fig. 5(a)], $3S \to 2\,^3P_1$ [Fig. 5(b)], or $3S \to 2\,^3P_0$ [Fig. 5(c)].

The transition (4.2) will be difficult to distinguish from (4.6), since the mean energies of the second and third photons in (4.2) are nearly the same as those of the third and second photons in (4.6). Some distinction may be possible on the basis of different patterns of Doppler broadening.

The transition (4.1) is expected to lead to a signal which is well isolated from any cascade involving $2S$ levels. This is our best candidate for detection of a $1D$ level. One looks for

$$E_{\gamma_1} \simeq 100 \text{ MeV} , \quad (4.7)$$

$$E_{\gamma_2} \simeq 100 \text{ MeV} , \quad (4.8)$$

$$E_{\gamma_3} \simeq 260 \text{ MeV} . \quad (4.9)$$

TABLE XI. Photon energies of all 3γ cascades from $3\,^3S_1$ down to $1\,^3P_J$.

$3\,^3S_1$			
$\to 2\,^3P_0 \to 2\,^3S_1 \to 1\,^3P_0$	124.25	205.00	162.26
$\to 1\,^3P_1$	124.25	205.00	130.64
$\to 1\,^3P_2$	124.25	205.00	109.50
$\to 1\,^3D_1 \to 1\,^3P_0$	124.25	81.18	285.08
$\to 1\,^3P_1$	124.25	81.18	253.84
$\to 1\,^3P_2$	124.25	81.18	232.96
$\to 2\,^3P_1 \to 2\,^3S_1 \to 1\,^3P_0$	99.32	229.67	162.26
$\to 1\,^3P_1$	99.32	229.67	130.64
$\to 1\,^3P_2$	99.32	229.67	109.50
$\to 1\,^3D_1 \to 1\,^3P_0$	99.32	106.14	285.08
$\to 1\,^3P_1$	99.32	106.14	253.84
$\to 1\,^3P_2$	99.32	106.14	232.96
$\to 1\,^3D_2 \to 1\,^3P_1$	99.32	99.22	260.67
$\to 1\,^3P_2$	99.32	99.22	239.80
$\to 2\,^3P_2 \to 2\,^3S_1 \to 1\,^3P_0$	86.54	242.27	162.26
$\to 1\,^3P_1$	86.54	242.27	130.64
$\to 1\,^3P_2$	86.54	242.27	109.50
$\to 1\,^3D_1 \to 1\,^3P_0$	86.54	118.90	285.08
$\to 1\,^3P_1$	86.54	118.90	253.84
$\to 1\,^3P_2$	86.54	118.90	232.96
$\to 1\,^3D_2 \to 1\,^3P_1$	86.54	111.98	260.67
$\to 1\,^3P_2$	86.54	111.98	239.80
$\to 1\,^3D_3 \to 1\,^3P_2$	86.54	107.04	244.68

TABLE XII. Combined branching ratios for three-photon cascades from $3S$ down to $1P$.

	$B1$ (%)	$B2$ (%)	$B3$ (%)	Combined (per million)
$3\,^3S_1$				
$\to 2\,^3P_0 \to 2\,^3S_1 \to 1\,^3P_0$	6.45	1.27	4.64	38
$\to 1\,^3P_1$	6.45	1.27	7.26	59
$\to 1\,^3P_2$	6.45	1.27	7.12	58
$\to 1\,^3D_1 \to 1\,^3P_0$	6.45	0.15	60.20	58
$\to 1\,^3P_1$	6.45	0.15	31.80	31
$\to 1\,^3P_2$	6.45	0.15	1.60	2
$\to 2\,^3P_1 \to 2\,^3S_1 \to 1\,^3P_0$	9.89	20.20	4.64	927
$\to 1\,^3P_1$	9.89	20.20	7.26	1450
$\to 1\,^3P_2$	9.89	20.20	7.12	1422
$\to 1\,^3D_1 \to 1\,^3P_0$	9.89	0.97	60.20	578
$\to 1\,^3P_1$	9.89	0.97	31.80	305
$\to 1\,^3P_2$	9.89	0.97	1.60	15
$\to 1\,^3D_2 \to 1\,^3P_1$	9.89	2.36	78.50	1832
$\to 1\,^3P_2$	9.89	2.36	20.30	474
$\to 2\,^3P_2 \to 2\,^3S_1 \to 1\,^3P_0$	10.90	10.10	4.64	511
$\to 1\,^3P_1$	10.90	10.10	7.26	799
$\to 1\,^3P_2$	10.90	10.10	7.12	784
$\to 1\,^3D_1 \to 1\,^3P_0$	10.90	0.02	60.20	13
$\to 1\,^3P_1$	10.90	0.02	31.80	7
$\to 1\,^3P_2$	10.90	0.02	1.60	0
$\to 1\,^3D_2 \to 1\,^3P_1$	10.90	0.29	78.50	248
$\to 1\,^3P_2$	10.90	0.29	20.30	64
$\to 1\,^3D_3 \to 1\,^3P_2$	10.90	1.42	95.40	1477

A useful "calibration" signal involves the cascade (4.3), in which

$$E_{\gamma_1} \simeq 100 \text{ MeV} , \tag{4.10}$$

$$E_{\gamma_2} \simeq 230 \text{ MeV} , \tag{4.11}$$

$$E_{\gamma_3} \simeq 130 \text{ MeV} . \tag{4.12}$$

2. *Angular distributions in three-photon cascades*

The angular distributions of photons in two-photon quarkonium cascade decays were discussed by many authors[35] around the time of the discovery of the decays $\psi' \to \gamma\chi \to \gamma\gamma J/\psi$. A more general formalism, drawn from lectures on nuclear physics,[36] is presented in the Appendix. Here we give only the main results.

Suppose, first of all, that a state with initial angular momentum J_i and magnetic quantum number M_i emits a photon with helicity λ and direction $\hat{\mathbf{k}}$ via j-pole radiation. If the polarization of the final state (with angular momentum J_f) is not observed, one finds a transition rate proportional to

$$\begin{aligned}\bar{w}(J_i M_i \to J_f; j\lambda\hat{\mathbf{k}}) &= \sum_R (-1)^{J_i - M_i - J_f - j + \lambda} \langle J_i J_i - M_i M_i \mid R0 \rangle \\ &\times \langle (jJ_f)J_i, (jJ_f)J_i; R \mid (jj)R, (J_f J_f)0; R \rangle \\ &\times (2R+1)^{-1/2} \langle jj - \lambda\lambda \mid R0 \rangle Y_0^R(\hat{\mathbf{k}}) . \end{aligned} \tag{4.13}$$

Here the only nontrivial quantity is the $9j$ coefficient, which can be expressed in terms of the standard $9j$ symbol

$$\langle (L_1 S_1)J_1, (L_2 S_2)J_2; J \mid (L_1 L_2)L, (S_1 S_2)S; J \rangle = \sqrt{(2J_1+1)(2J_2+1)(2L+1)(2S+1)} \begin{Bmatrix} L_1 & S_1 & J_1 \\ L_2 & S_2 & J_2 \\ L & S & J \end{Bmatrix} . \tag{4.14}$$

One may simplify Eq. (4.13) further by summing over photon polarizations $\lambda = \pm 1$, whereby only even values of R [$\leq \min(2J_i, 2j)$ in any case] enter into the sum. For an initial $^3S_1$ state produced via e^+e^- annihilations one also sums over $M_i = \pm 1$. The well-known results for $^3S_1 \to \gamma + {}^3P_J$ $E1$ transitions are then a special case of Eq. (4.13) with $j=1$, summed over $M_i = \pm 1$, $\lambda = \pm 1$, $R = 0, 2$:

$$w(^3S_1 \to \gamma + {}^3P_0) \sim 1 + \cos^2\theta , \tag{4.15}$$

$$w(^3S_1 \to \gamma + {}^3P_1) \sim 1 - \tfrac{1}{3}\cos^2\theta , \tag{4.16}$$

$$w(^3S_1 \to \gamma + {}^3P_2) \sim 1 + \tfrac{1}{13}\cos^2\theta . \tag{4.17}$$

Here θ is the angle of the photon with respect to the e^+e^- beam axis.

For multiphoton cascades, Eq. (4.13) has a straightforward generalization. For example, if three photons with $j_i, \lambda_i, \hat{\mathbf{k}}_i$ $(i = 1,2,3)$ are emitted in the cascade

$$(J_i, M_i) \xrightarrow{\gamma_1} (J_a, M_a) \xrightarrow{\gamma_2} (J_b, M_b) \xrightarrow{\gamma_3} (J_f, M_f) , \tag{4.18}$$

and the polarizations M_a, M_b, M_f are summed over, the transition rate is proportional to

$$\begin{aligned}\bar{w}(J_i M_i \to (J_a, J_b) \to J_f; j_1\lambda_1\hat{\mathbf{k}}_1, j_2\lambda_2\hat{\mathbf{k}}_2, j_3\lambda_3\hat{\mathbf{k}}_3) &= \sum_{\substack{K_1 K_2 K_3 \\ IR}} \langle J_i J_i - M_i M_i \mid R0 \rangle (-1)^{J_i - M_i} \prod_{n=1}^{3} (-1)^{\lambda_n - j_n} (2K_n + 1)^{-1/2} \langle j_n j_n - \lambda_n \lambda_n \mid K_n 0 \rangle \\ &\times \langle J_a j_1)J_i, (J_a j_1)J_i; R \mid (J_a J_a)I, (j_1 j_1)K_1; R \rangle \\ &\times \langle (J_b j_2)J_a, (J_b j_2)J_a; I \mid (J_b J_b)K_3, (j_2 j_2)K_2; I \rangle \\ &\times \langle (J_f j_3)J_b, (J_f j_3)J_b; K_3 \mid (J_f J_f)0, (j_3 j_3)K_3; K_3 \rangle \\ &\times [[Y^{K_3}(\hat{\mathbf{k}}_3) Y^{K_2}(\hat{\mathbf{k}}_2)]^I Y^{K_1}(\hat{\mathbf{k}}_1)]_0^R . \end{aligned} \tag{4.19}$$

Here the notation $[\psi^{J_1}\psi^{J_2}]^J_M$ is shorthand for

$$[\psi^{J_1}\psi^{J_2}]^J_M=\sum_{m_1m_2}\langle J_1J_2m_1m_2\,|\,JM\rangle\psi^{J_1}_{m_1}\psi^{J_2}_{m_2}\ , \tag{4.20}$$

so that

$$[[Y^{K_3}(\hat{\mathbf{k}}_3)Y^{K_2}(\hat{\mathbf{k}}_2)]^IY^{K_1}(\hat{\mathbf{k}}_1)]^R_0=\sum_{m_1m_2m_3}\langle K_3K_2m_3m_2\,|\,I-m_1\rangle\langle IK_1-m_1m_1\,|\,R0\rangle Y^{K_3}_{m_3}(\hat{\mathbf{k}}_3)Y^{K_2}_{m_2}(\hat{\mathbf{k}}_2)Y^{K_1}_{m_1}(\hat{\mathbf{k}}_1)\ . \tag{4.21}$$

For the case of present interest, we assume that a $3\,^3S_1$ state is produced via e^+e^- annihilations and decays via electric dipole transitions through a three-photon cascade to $1\,^3P_{J_f}$. We assume that all photon polarizations and M_a,M_b,M_f are summed over, and also sum over $M_i=\pm1$. We then find

$$\begin{aligned}\bar{w}(3\,^3S_1\to(J_aJ_b)\to1\,^3P_{J_f};\hat{\mathbf{k}}_1\hat{\mathbf{k}}_2\hat{\mathbf{k}}_3)&\\ =\sum_{K_1K_2K_3}\langle11-11\,|\,R0\rangle\prod_{n=1}^{3}\langle11-11\,|\,K_n0\rangle\frac{1}{\sqrt{2K_n+1}}&\\ \times\langle(J_a1)1,(J_a1)1;R\,|\,(J_aJ_a)I;(11)K_1;R\rangle\langle(J_b1)J_a,(J_b1)J_a;I\,|\,(J_bJ_b)K_3,(11)K_2;I\rangle&\\ \times\langle(J_f1)J_b,(J_f1)J_b;K_3\,|\,(J_fJ_f)0,(11)K_3;K_3\rangle[[Y^{K_3}(\hat{\mathbf{k}}_3)Y^{K_2}(\hat{\mathbf{k}}_2)]^IY^{K_1}(\hat{\mathbf{k}}_1)]^R_0\ ,&\end{aligned} \tag{4.22}$$

where $K_1,K_2,K_3,R=0,2$ and $I=0,2,4\le\min(2J_a,K_2+K_3)$. Here

$$\begin{aligned}[[Y^{K_3}(\hat{\mathbf{k}}_3)Y^{K_2}(\hat{\mathbf{k}}_2)]^IY^{K_1}(\hat{\mathbf{k}}_1)]^R_0=(4\pi)^{-3/2}\sum_{m_1m_2m_3}\langle K_3K_2m_3m_2\,|\,I-m_1\rangle\langle IK_1-m_1m_1\,|\,R0\rangle&\\ \times G_{K_3m_3}(\theta_3)G_{K_2m_2}(\theta_2)G_{K_1m_1}(\theta_1)\cos(m_1\phi_1+m_2\phi_2+m_3\phi_3)\ ,&\end{aligned} \tag{4.23}$$

and $G_{00}(\theta)=1$, $G_{22}(\theta)=\sqrt{15/8}\sin^2\theta$, $G_{21}(\theta)=-\sqrt{15/2}\sin\theta\cos\theta$, $G_{20}(\theta)=\sqrt{5/4}(3\cos^2\theta-1)$, with $G_{k-m}(\theta)=(-1)^mG_{km}(\theta)$. For $\bar{w}$ in Eq. (4.22) to be normalized to one, it must be multiplied by the factor $N\equiv\sqrt{(2J_f+1)/3}(4\pi/9)^{-3/2}$, whereupon

$$\int\bar{w}N\,d\Omega_{\hat{\mathbf{k}}_1}d\Omega_{\hat{\mathbf{k}}_2}d\Omega_{\hat{\mathbf{k}}_3}=1\ . \tag{4.24}$$

If one integrates over the azimuthal angles of the photons, one finds

$$\int[[Y^{K_3}(\hat{\mathbf{k}}_3)Y^{K_2}(\hat{\mathbf{k}}_2)]^IY^{K_1}(\hat{\mathbf{k}}_1)]^R_0d\phi_1d\phi_2d\phi_3=(2\pi)^3(4\pi)^{-3/2}\langle K_3K_200\,|\,I0\rangle\langle IK_100\,|\,R0\rangle G_{K_10}(\theta_1)G_{K_20}(\theta_2)G_{K_30}(\theta_3)\ . \tag{4.25}$$

We have calculated distributions in θ_1, θ_2, and θ_3, integrated over azimuthal angles, to gain an idea of the variation in signal to be expected for various cascades over different portions of a detector with axial symmetry. For purpose of display, we chose fixed values of $\theta_1=0°,60°,90°$ and plotted contours of signal strength with respect to θ_2 and θ_3. Some results are shown in Figs. 6 and 7. Variations in strength are not appreciable (especially since $K_i\le2$, leading to polynomials of at most second order in $\cos\theta_i$). Nonetheless, characteristic differences can be seen among transitions. It may be possible to apply our results to discriminate among various spin-parity assignments.

3. *Four-photon transitions to* $\Upsilon(1S)$

The results of Table XII show that statistics of three-photon cascades from $\Upsilon(3S)$ are not a limiting factor, since present samples of produced $\Upsilon(3S)$ exceed 5.8×10^5 (Ref. 4). Backgrounds may be severe, however. The four-photon cascades illustrated in Fig. 8, followed by $\Upsilon(1S)\to l^+l^-$, have only the background $\Upsilon(3S)\to\pi^0\pi^0\Upsilon(1S)$, which is expected to occur with a branching ratio of about 2%. The three-photon cascades in Table XI which end up in $1\,^3P_1$ states are expected to yield a fourth photon $(\gamma_4)+\Upsilon(1S)$ 46.1% of the time, while those populating $1\,^3P_2$ states give $\gamma_4+\Upsilon(1S)$ 22.2% of the time. Altogether from $10^6\Upsilon(3S)$ we expect the transitions

$$3S\overset{\gamma_1}{\to}2P\overset{\gamma_2}{\to}2S\overset{\gamma_3}{\to}1P\overset{\gamma_4}{\to}1S \tag{4.26}$$

and

$$3S\overset{\gamma_1}{\to}2P\overset{\gamma_2}{\to}1D\overset{\gamma_3}{\to}1P\overset{\gamma_4}{\to}1S \tag{4.27}$$

each to yield somewhat over 1600 $\Upsilon(1S)$, to be compared with somewhat under 20 000 from $\Upsilon(3S)\to\pi^0\pi^0\Upsilon(1S)$.

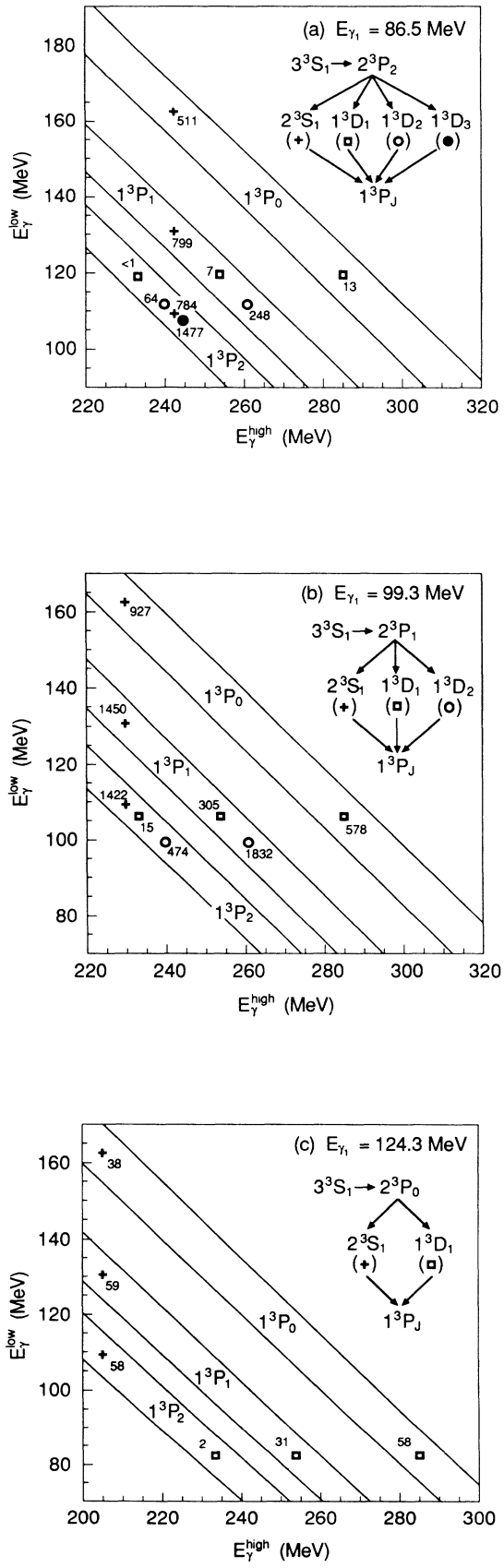

FIG. 5. Expected numbers of events as function of second and third photon energies for the cascades illustrated in Fig. 3. (a) $3S \rightarrow 2\,^3P_2$, (b) $3S \rightarrow 2\,^3P_1$, (c) $3S \rightarrow 2\,^3P_0$.

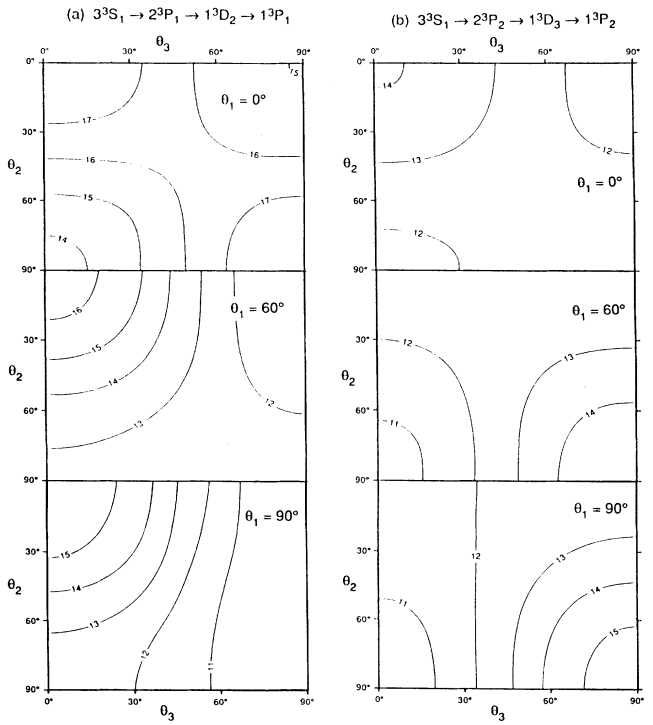

FIG. 6. Contours of relative photon intensities for $3S \rightarrow 2P \rightarrow 1D \rightarrow 1P$ transitions. (a) $3S \rightarrow 2\,^3P_1 \rightarrow 1\,^3D_2 \rightarrow 1\,^3P_1$ [Eq. (4.1)], (b) $3S \rightarrow 2\,^3P_2 \rightarrow 1\,^3D_3 \rightarrow 1\,^3P_2$ [Eq. (4.2)].

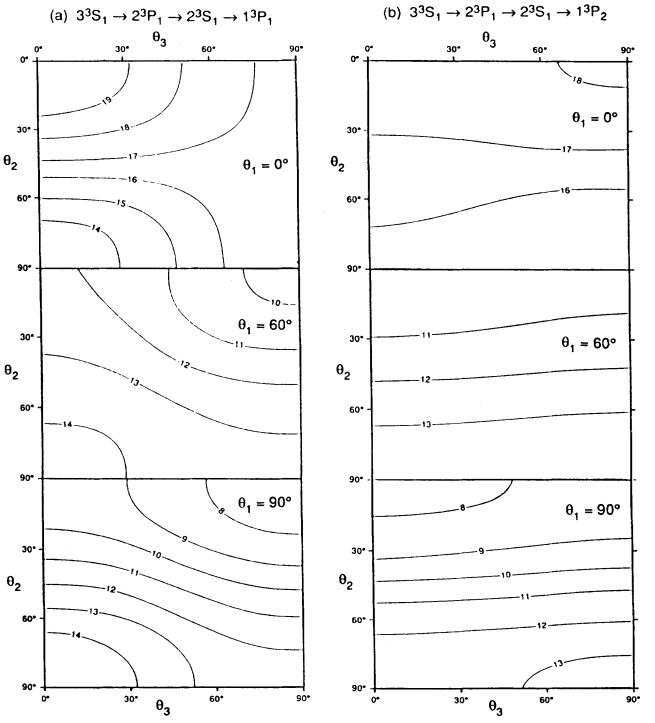

FIG. 7. Contours of relative photon intensities for $3S \rightarrow 2P \rightarrow 2S \rightarrow 1P$ transitions. (a) $3S \rightarrow 2\,^3P_1 \rightarrow 2S \rightarrow 1\,^3P_1$ [Eq. (4.3)], (b) $3S \rightarrow 2\,^3P_1 \rightarrow 2S \rightarrow 1\,^3P_2$ [Eq. (4.4)].

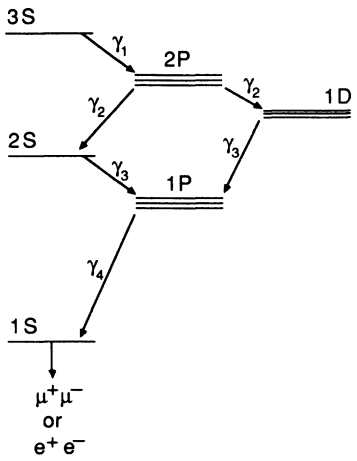

FIG. 8. Scheme of transitions in four-photon cascades from the Υ(3S).

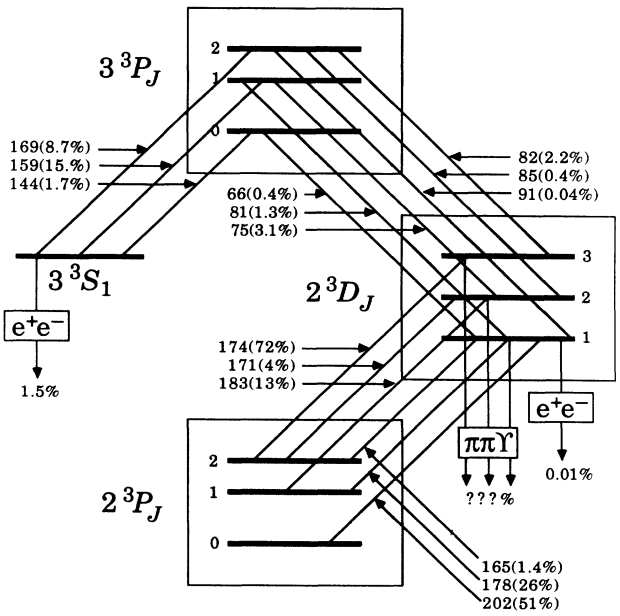

FIG. 9. Branching ratios for radiative transitions from the $3\,^3P$ $b\bar{b}$ levels.

The Υ(1S) is detected via its $l^+l^-=(e^+e^-$ or $\mu^+\mu^-)$ decays, corresponding to a branching ratio of 5.6%. If $\pi^0\pi^0\Upsilon$ events can be excluded without significant loss in statistics, the four-photon cascades may be just at the limit of detectability.

B. Hadronic production of *D* states

The Υ(1S), Υ(2S), and Υ(3S) were first discovered in hadronic reactions,[37] and now have been studied there with excellent statistics and mass resolution.[5] It is thought (see, e.g., Ref. 38) that at least some of the observed hadronic production of Υ levels proceeds via the two-gluon formation of $C=+$ $b\bar{b}$ levels, which then decay to $\gamma+n\,^3S_1$ states. The presence of Υ(3S) then supports the prediction (see Fig. 1) that the $3P$ $b\bar{b}$ levels are below flavor threshold.

If $2P$ and $3P$ $b\bar{b}$ levels are being produced hadronically, they are able to decay electromagnetically to D states as well as to S states. For the $2P$ levels, the relative branching ratios have already been illustrated in Fig. 4. In Fig. 9 we show a corresponding comparison for the $3P$ levels. The branching ratios of the $3\,^3P$ levels have been calculated using the radiative decay widths quoted in Tables VII(b) and VII(c). We have included only electromagnetic decays $2D\to 1P$, $2P$, and $1F$ in calculations of the $2D$ branching ratios. Omitted processes, expected to make small contributions, include $2D\to\pi\pi+(b\bar{b})$ and $2D\to 3$ gluons decays.

The best hope for detecting D states in hadronic reactions may lie in the extremely rare decay modes $^3D_1\to e^+e^-$, $\mu^+\mu^-$. The branching ratios for these decays have been included in Figs. 4 and 12. Observation of these decays will require greater sensitivities than achieved at present. Very roughly, we see from Fig. 9 that the electromagnetic transitions $3P\to 2D$ occur at a rate no more than 10% of $3P\to 3S$, and the branching ratio of $2\,^3D_1$ to e^+e^- is about 10^{-2} of that for $3S\to e^+e^-$. Thus, we might expect to see about one $2\,^3D_1\to e^+e^-$ decay for every 10^3 $3S\to e^+e^-$ decays in hadronic reactions such as those described in Ref. 5. The recent calculation[33] of very small $\pi\pi\Upsilon$ widths for D states makes their detection in $\pi\pi\Upsilon$ final states less likely than proposed in Ref. 1.

C. *D*-states in direct e^+e^- annihilations

Energy scans have been performed in e^+e^- annihilations around the masses of the proposed $^3D_1$ levels. At present their limits[39] are about a factor of 10 above present expectations[21] for $\Gamma_{ee}(1\,^3D_1,2\,^3D_1)=(1.5,2.7)$ eV. Those expectations included tensor force mixing with S states, but not coupled-channel effects.[40] However, such effects are expected to be much less important for the $1\,^3D_1$ and $2\,^3D_1$ levels of $b\bar{b}$ than for the $1\,^3D_1$ $c\bar{c}$ level [ψ''(3770)], which lies above flavor threshold and in fact is observed to be substantially mixed with $^3S_1$ levels [particularly ψ'(3686)].

D. *D*-states of the $c\bar{c}$ system

Although it is not our purpose here to discuss D-wave $c\bar{c}$ levels, which require a careful treatment of coupled-channel effects[40] since they nearly all lie above flavor threshold, it is important to point out a few implications of recent results[32,33] for such levels.

(1) The decays of ψ''(3770) to $\pi\pi+J/\psi$ are expected to be negligible for a pure D state.[33,34] Thus, the decay $\psi''\to\pi\pi+J/\psi$ can be a useful indication of S-state admixtures in the ψ''.

(2) A purely D-wave ψ''(3770) has an extremely small decay width to χ_2, as one sees from the entry for $^3D_1\to{}^3P_2$ in Table VI. Observation of such a decay, and

comparison with the widths for $\psi'' \to \gamma\chi_2$, $\gamma\chi_1$, and $\gamma\chi_0$ can further pinpoint S-D mixing in the ψ''.

(3) The $c\bar{c}$ levels $1\,^3D_2$ and $1\,^1D_2$ are expected to be below flavor threshold, since they are expected[41] to be slightly too low in mass to decay to $D\bar{D}^*(+\text{c.c.})$, while their $D\bar{D}$ decay is forbidden by parity and angular momentum conservation. Proposals[42] to produce these levels in $\bar{p}p$ collisions will take advantage of this fact. The dominant decays of $1\,^3D_2$ should be to $\gamma + \chi(1\,^3P_{1,2})$, while that of $1\,^1D_2$ should be to $\gamma + h_c\,(1\,^1P_1)$.

V. CONCLUSIONS

We have investigated properties of the D-wave levels of the Υ family and have made suggestions for their observation. The centers of gravity of the $1D$ and $2D$ multiplets are expected to lie around 10.16 and 10.44 GeV/c^2, respectively. The best prospects for observing the $1D$ levels appear to be their production via electromagnetic cascades from the $\Upsilon(3S)$. The $1\,^3D_1$ and $2\,^2D_1$ levels also may be observable in high-statics hadronic reactions via their e^+e^- or $\mu^+\mu^-$ decays, and via direct scans in e^+e^- annihilations at levels sensitive to the predicted leptonic widths of 1.5 and 2.7 eV, respectively.

ACKNOWLEDGMENTS

We are grateful to Juliet Lee-Franzini and John Rutherfoord for stimulation and encouragement, and Marina Artuso, Kuang-ta Chao, Richard Galik, and David Hitlin for helpful discussions. This work was supported in part by the Department of Energy, Grant No. DE-AC02-80ER-10587.

APPENDIX: ANGULAR DISTRIBUTIONS

In this appendix we will sketch the derivation of the angular distribution for triple cascade, Eq. (4.19). The state vector for vector mesons can be labeled by the ket $|\,n(LS)JM\,\rangle$. In order to make the spatial dependence of the state more explicit, we will adopt the equivalent notation $\Psi^J_{nM}(\mathbf{r})$, with

$$|\,\Psi^J_{nM}(\mathbf{r})\,\rangle = |\,[\psi^L_n(\mathbf{r})\chi^S]^J_M\,\rangle \equiv |\,n(LS)JM\,\rangle\ , \tag{A1}$$

where the quantum numbers L and S have been suppressed, and $\psi^L_{nM_L}(\mathbf{r})$ and $\chi^S_{M_S}$ are respectively the spatial and spin wave function of the meson state. Ψ^J_M decomposes into $\psi^L_{M_L}$ and $\chi^S_{M_S}$ according to the usual rule of addition of angular momentum:

$$\Psi^J_M = \sum_{M_L,M_S} \langle LSM_LM_S\,|\,JM\,\rangle \psi^L_{M_L}\chi^S_{M_S} = [\psi^L\chi^S]^J_M\ . \tag{A2}$$

Suppose a meson in the state $\Psi^{J_i}_{M_i}(\mathbf{r})$ decays to some other states by the emission of a j-pole photon with helicity λ and wave vector $\mathbf{k}$. The wave function of the photon in momentum space is proportional to $D^{*J}_{m\lambda}(\mathbf{k})$. If we assume that $\Psi^n_{M_n}(\mathbf{r})$, $n=1,2,3,\ldots$ form a complete basis, then the action of the interaction Hamiltonian on $\Psi^{J_i}_{M_i}(\mathbf{r})$ must yield

$$H_{\text{int}}\,|\,\Psi^{J_i}_{M_i}(\mathbf{r})\,\rangle = \sum_n C_{in}\,|\,[D^{*j}_{,\lambda}(\hat{\mathbf{k}})\Psi^{J_n}(\mathbf{r})]^{J_i}_{M_i}\,\rangle\ , \tag{A3}$$

where C_{in} are a set of coefficients specified by details of the interaction. The transition amplitude into a specific final state $\Psi^{J_f}_{M_f}(\mathbf{r})$ is the projection of this state into $|\,\Psi^{J_f}_{M_f}(\mathbf{r})\,\rangle$ which will pick out the term with $J_n = J_f$ and is proportional to

$$\langle\,\Psi^{J_f}_{M_f}(\mathbf{r})\,|\,[D^{*j}_{,\lambda}(\hat{\mathbf{k}})\Psi^{J_f}_{M_f}(\mathbf{r})]^{J_i}_{M_i}\,\rangle = \int d^3r\,\Psi^{J_f}_{M_f}(\mathbf{r})[D^{*j}_{,\lambda}(\hat{\mathbf{k}})\Psi^{J_f}_{M_f}(\mathbf{r})]^{J_i}_{M_i}\ . \tag{A4}$$

The square of this amplitude gives us the transition rate

$$w(J_iM_i \to J_fM_f; j\lambda\hat{\mathbf{k}}) = \int d^3r_1 d^3r_2 \Psi^{*J_f}_{M_f}(\mathbf{r}_1)\Psi^{J_f}_{M_f}(\mathbf{r}_2)[D^{*j}_{,\lambda}(\hat{\mathbf{k}})\Psi^{J_f}(\mathbf{r}_2)]^{*J_i}_{M_i}[D^{*j}_{,\lambda}(\hat{\mathbf{k}})\Psi^{J_f}(\mathbf{r}_1)]^{J_i}_{M_i}\ . \tag{A5}$$

Assuming real radial wave functions, we have

$$\Psi^{*J}_M = (-1)^M\Psi^J_{-M}\ , \tag{A6}$$

$$D^j_{m\lambda} = (-1)^{\lambda-m}D^{*j}_{-m,-\lambda}\ , \tag{A7}$$

so that

$$\Psi^{*J_f}_{M_f}(\mathbf{r}_1)\Psi^{J_f}_{M_f}(\mathbf{r}_2) = (-1)^{M_f}\Psi^{J_f}_{-M_f}(\mathbf{r}_1)\Psi^{J_f}_{M_f}(\mathbf{r}_2) = \sum_{R'}(-1)^{M_f}\langle J_fJ_f - M_fM_f\,|\,R'0\rangle[\Psi^{J_f}(\mathbf{r}_1)\Psi^{J_f}(\mathbf{r}_2)]^{R'}_0\ . \tag{A8}$$

Similarly

$$[D^{*j}_{,\lambda}(\hat{\mathbf{k}})\Psi^{J_f}(\mathbf{r}_2)]^{*J_i}_{M_i}[D^{*j}_{,\lambda}(\hat{\mathbf{k}})\Psi^{J_f}(\mathbf{r}_1)]^{J_i}_{M_i} = \sum_R(-1)^{J_i-j-J_f+\lambda-M_i}\langle J_iJ_i - M_iM_i\,|\,R0\rangle \times[[D^{*j}_{,-\lambda}(\hat{\mathbf{k}})\Psi^{J_f}(\mathbf{r}_2)]^{J_i}[D^{*j}_{,\lambda}(\hat{\mathbf{k}})\Psi^{J_f}(\mathbf{r}_1)]^{J_i}]^R_0\ . \tag{A9}$$

The four wave functions in Eq. (A9) can be recoupled to a different order to give

$$[[D^{*j}_{,-\lambda}\Psi^{J_f}]^{J_i}[D^{*j}_{,\lambda}\Psi^{J_f}]^R_0=\sum_{K,I}\langle (jJ_f)J_i,(jJ_f)J_i;R\mid (jj)K,(J_fJ_f)I;R\rangle[[D^{*J}_{,-\lambda}D^{*j}_{,\lambda}]^K[\Psi^{J_f}\Psi^{J_f}]^I]^R_0 \tag{A10}$$

and

$$[D^{*j}_{,-\lambda}(\hat{\mathbf{k}})D^{*j}_{,\lambda}(\hat{\mathbf{k}})]^K_M=\langle jj-\lambda\lambda\mid K0\rangle D^{*K}_{M0}(\hat{\mathbf{k}})=\langle jj-\lambda\lambda\mid K0\rangle\left[\frac{4\pi}{2K+1}\right]^{1/2}Y^K_M(\hat{\mathbf{k}})\ . \tag{A11}$$

The rate thus becomes

$$\begin{aligned}w=\int d^3r_1d^3r_2\sum_{RR'}(-1)^{M_f}\langle J_fJ_f-M_fM_f\mid R'0\rangle[\Psi^{J_f}(\mathbf{r}_1)\Psi^{J_f}(\mathbf{r}_2)]^{R'}_0(-1)^{J_i-j-J_f+\lambda-M_i}\langle J_iJ_i-M_iM_i\mid R0\rangle\\ \times\sum_{K,I}\langle (jJ_f)J_i,(jJ_f)J_i;R\mid (jj)K,(J_fJ_f)I;R\rangle\\ \times\langle jj-\lambda\lambda\mid K0\rangle\left[\frac{2\pi}{2K+1}\right]^{1/2}[Y^K(\hat{\mathbf{k}})[\Psi^{J_f}(\mathbf{r}_2)\Psi^{J_f}(\mathbf{r}_1)]^I]^R_0\ .\end{aligned} \tag{A12}$$

If we do not measure the polarization of the final states, then summing over M_f gives

$$\sum_{M_f}(-1)^{J_f+M_f}\langle J_fJ_f-M_fM_f\mid R'0\rangle=\sqrt{2J_f+1}\delta_{R',0}\ . \tag{A13}$$

Also

$$\int d^3r_1d^3r_2[\Psi^{J_f}(\mathbf{r}_1)\Psi^{J_f}(\mathbf{r}_2)]^0_0[\Psi^{J_f}(\mathbf{r}_2)\Psi^{J_f}(\mathbf{r}_1)]^I_{M_I}=\delta_{I,0}\delta_{M_I,0}\ . \tag{A14}$$

Dropping all radial factors and overall constants, we obtain the angular distribution $\bar{w}(J_iM_i\to J_f;j\lambda\hat{\mathbf{k}})$:

$$\bar{w}=\sum_R(-1)^{\lambda-M_i}\langle J_iJ_i-M_iM_i\mid R0\rangle\langle (jJ_f)J_i,(jJ_f)J_i;R\mid (jj)R,(J_fJ_f)0;R\rangle(2R+1)^{-1/2}\langle jj-\lambda\lambda\mid R0\rangle Y^R_0(\hat{\mathbf{k}})\ . \tag{A15}$$

To generalize this to the successive emission of three photons, let us consider the cascade (4.18):

$$(J_iM_i)\overset{\gamma_1}{\to}(J_aM_a)\overset{\gamma_2}{\to}(J_bM_b)\overset{\gamma_3}{\to}(J_fM_f)\ . \tag{4.18}$$

Each γ_i has quantum number $j_i,\lambda_i,\mathbf{k}_i$. The total final state of this cascade will be proportional to

$$[[[D^{*j_3}_{,\lambda_3}(\hat{\mathbf{k}}_3)\Psi^{J_f}(\mathbf{r})]^{J_b}D^{*j_2}_{,\lambda_2}(\hat{\mathbf{k}}_2)]^{J_a}D^{*j_1}_{,\lambda_1}(\hat{\mathbf{k}}_1)]^{J_i}_{M_i}\ . \tag{A16}$$

The transition probability into the state $\Psi^{J_f}_{M_f}(\mathbf{r})$ will contain (A16) and its complex conjugate and hence the factor

$$[[[D^{*j_3}_{,-\lambda_3}(\hat{\mathbf{k}}_3)\Psi^{J_f}(\mathbf{r}')]^{J_b}D^{*j_2}_{,-\lambda_2}(\hat{\mathbf{k}}_2)]^{J_a}D^{*j_1}_{,-\lambda_1}(\hat{\mathbf{k}}_1)]^{J_i}_{-M_i}[D^{*j_3}_{,\lambda_3}(\hat{\mathbf{k}}_1)\Psi^{J_f}(\mathbf{r})]^{J_b}D^{*j_2}_{,\lambda_2}(\hat{\mathbf{k}}_2)]^{J_2}D^{*j_1}_{,\lambda_1}(\hat{\mathbf{k}}_1)]^{J_a}_{M_a}\ . \tag{A17}$$

The D^{*J_i}'s with the same argument can be grouped together by recoupling (A17) three times, each time bringing in one $9j$ coefficient and a factor of $(2K_i+1)^{-1/2}\langle j_ij_i-\lambda_i\lambda_i\mid K_i0\rangle$ for expressing $[D^{*j_i}_{,-\lambda_i}(\hat{\mathbf{k}}_i)D^{*j_i}_{,\lambda_i}(\hat{\mathbf{k}}_i)]^{K_i}_M$ in terms of $Y^{K_i}_M(\hat{\mathbf{k}}_i)$. Collecting all factors and summing over M_f, we obtain Eq. (4.19):

$$\begin{aligned}&\bar{w}(J_iM_i\to(J_a,J_b)\to J_f;j_1\lambda_1\hat{\mathbf{k}}_1,j_2\lambda_2\hat{\mathbf{k}}_2,j_3\lambda_3\hat{\mathbf{k}}_3)\\ &=\sum_{\substack{K_1K_2K_3\\IR}}\langle J_iJ_i-M_iM_i\mid R0\rangle(-1)^{J_i-M_i}\prod_{n=1}^3(-1)^{\lambda_n-j_n}(2K_n+1)^{-1/2}\langle j_nj_n-\lambda_n\lambda_n\mid K_n0\rangle\\ &\quad\times\langle (J_aj_1)J_i,(J_aj_1)J_i;R\mid (J_aJ_a)I,(j_1j_1)K_1;R\rangle\\ &\quad\times\langle (J_bj_2)J_a,(J_bj_2)J_a;I\mid (J_bJ_b)K_3,(j_2j_2)K_2;I\rangle\\ &\quad\times\langle (J_fj_3)J_b,(J_fj_3)J_b;K_3\mid (J_fJ_f)0,(j_3j_3)K_3;K_3\rangle\\ &\quad\times[[Y^{K_3}(\hat{\mathbf{k}}_3)Y^{K_2}(\hat{\mathbf{k}}_2)]^IY^{K_1}(\hat{\mathbf{k}}_1)]^R_0\ ,\end{aligned} \tag{4.19}$$

where

$$[[Y^{K_3}(\hat{\mathbf{k}}_3)Y^{K_2}(\hat{\mathbf{k}}_2)]^I Y^{K_1}(\hat{\mathbf{k}}_1)]_0^R = \sum_{m_1 m_2 m_3} \langle K_3 K_2 m_3 m_2 \mid I - m_1 \rangle \langle I K_1 - m_1 m_1 \mid R 0 \rangle Y_{m_3}^{K_3}(\hat{\mathbf{k}}_3) Y_{m_2}^{K_2}(\hat{\mathbf{k}}_2) Y_{m_1}^{K_1}(\hat{\mathbf{k}}_1) \ . \quad (4.21)$$

All the intermediate angular momenta satisfy the following vector addition formulas:

$$\begin{aligned} &\mathbf{K}_n = \mathbf{j}_n + \mathbf{j}_n \ , \quad n = 1,2,3 \ , \\ &\mathbf{I} = \mathbf{K}_2 + \mathbf{K}_3 = \mathbf{J}_a + \mathbf{J}_a \ , \quad \mathbf{K}_1 + \mathbf{K}_2 + \mathbf{K}_3 = \mathbf{R} = \mathbf{J}_i + \mathbf{J}_i \ . \end{aligned} \quad (A18)$$

[1]Waikwok Kwong, Jonathan L. Rosner, and Chris Quigg, Annu. Rev. Nucl. Part. Sci. **37**, 325 (1987).

[2]Chris Quigg, in *Proceedings of the 1979 International Symposium on Lepton and Photon Interactions at High Energy,* Fermilab, 1979, edited by T. B. W. Kirk and H. D. I. Abarbanel (Fermilab, Batavia, Illinois, 1979), p. 239.

[3]M. B. Voloshin, Yad. Fiz. **36**, 247 (1982) [Sov. J. Nucl. Phys. **36**, 143 (1982)].

[4]For a recent review, see J. Lee-Franzini, in *Proceedings of the International Symposium on Lepton and Photon Interactions at High Energies,* Hamburg, 1987, edited by W. Bartel and R. Rückl (Nucl. Phys. B, Proc. Suppl., Vol. 3) (North-Holland, Amsterdam, 1988), p. 139.

[5]Fermilab Experiment No. E-605, C. N. Brown *et al.*, in *Proceedings of the Second Aspen Winter Particle Physics Conference,* edited by L. Durand (New York Academy of Sciences, New York, 1987); Ann. N.Y. Acad. Sci. **490**, 181 (1987); D. M. Kaplan, in *Quarks, Strings, Dark Matter and All the Rest,* proceedings of the 7th Vanderbilt High Energy Physics Conference, Nashville, 1986, edited by R. Panvini and T. Weiler (World Scientific, Singapore, 1987), p. 83.

[6]H. B. Thacker, C. Quigg, and Jonathan L. Rosner, Phys. Rev. D **18**, 274 (1978); **18**, 287 (1978).

[7]C. Quigg, H. B. Thacker, and Jonathan L. Rosner, Phys. Rev. D **21**, 234 (1980).

[8]C. Quigg and Jonathan L. Rosner, Phys. Rev. D **23**, 2625 (1981); Peter Moxhay, Jonathan L. Rosner, and C. Quigg, *ibid.* **23**, 2638 (1981).

[9]B. Baumgartner, H. Grosse, and A. Martin, Nucl. Phys. **B254**, 528 (1985).

[10]C. V. Sukamar, J. Phys. A **18**, L57 (1985); **18**, 2917 (1985); **18**, 2937 (1985); **19**, 2229 (1986); **19**, 2297 (1986).

[11]Waikwok Kwong and Jonathan L. Rosner, Prog. Theor. Phys. Suppl. **86**, 366 (1986) (Festschrift volume in honor of Y. Nambu).

[12]Jonathan F. Schonfeld, Waikwok Kwong, Jonathan L. Rosner, C. Quigg, and H. B. Thacker, Ann. Phys. (N.Y.) **128**, 1 (1980).

[13]Waikwok Kwong, Jonathan L. Rosner, Jonathan F. Schonfeld, C. Quigg, and H. B. Thacker, Am. J. Phys. **48**, 926 (1980).

[14]W. Buchmüller, Phys. Lett. **112B**, 479 (1982); in *Fundamental Interactions in Low Energy Systems,* proceedings of the Fourth Course of the International School of Physics, Erice, Italy, 1984, edited by P. Dalpiaz, G. Fiorentini, and G. Torelli (Ettore Majorana International Science Series: Physical Sciences, Vol. 23) (Plenum, New York, 1985). For further references to this model, motivated by a rotating tube of chromoelectric flux, see E. Eichten and F. Feinberg, Phys. Rev. D **23**, 2724 (1981); D. Z. Gromes, Z. Phys. C **26**, 401 (1984).

[15]G. Darboux, C. R. Acad. Sci. (Paris) **94**, 1456 (1882).

[16]E. Witten, Nucl. Phys. **B188**, 513 (1981); F. Cooper and B. Freedman, Ann. Phys. (N.Y.) **146**, 262 (1983); L. E. Gendenshtein, Pis'ma Zh. Eksp. Teor. Fiz. **38**, 299 (1983) [JETP Lett. **38**, 356 (1983)]; M. M. Nieto, Phys. Lett. **145B**, 208 (1984); M. Bernstein and L. S. Brown, Phys. Rev. Lett. **52**, 1933 (1984); V. A. Kostelecký and M. M. Nieto, *ibid.* **53**, 2285 (1984); T. D. Imbo and V. P. Sukhatme, *ibid.* **54**, 2184 (1985); M. Luban and D. L. Pursey, Phys. Rev. D **33**, 431 (1986).

[17]Particle Data Group, M. Aguilar-Benitez *et al.*, Phys. Lett. **170B**, 1 (1986).

[18]See, e.g., Susan Cooper, in *Proceedings of the XXIII International Conference on High Energy Physics,* Berkeley, California, 1986, edited by S. Loken (World Scientific, Singapore, 1987), p. 67; Lee-Franzini (Ref. 4).

[19]Waikwok Kwong, Paul B. Mackenzie, Rogerio Rosenfeld, and Jonathan L. Rosner, Phys. Rev. D **37**, 3210 (1988).

[20]E. Eichten *et al.*, Phys. Rev. D **21**, 203 (1980); E. Eichten, in *Dynamics and Spectroscopy at High Energy,* proceedings of the 11th SLAC Summer Institute on Particle Physics, Stanford, California, 1983, edited by P. M. McDonough (SLAC Report No. 267, Stanford, 1984), p. 497; W. Buchmüller and S.-H. H. Tye. Phys. Rev. D **24**, 132 (1981).

[21]Peter J. Moxhay and Jonathan L. Rosner, Phys. Rev. D **28**, 1132 (1983); Peter Jack Moxhay, thesis, University of Minnesota, 1983.

[22]S. N. Gupta, S. Radford, and W. Repko, Phys. Rev. D **26**, 3305 (1982); **30**, 2424 (1984); Phys. Rev. Lett. **55**, 3006 (1985); Phys. Rev. D **31**, 160 (1985); **34**, 201 (1986).

[23]Jonathan L. Rosner, in *Proceedings of the International Symposium on Lepton and Photon Interactions at High Energy,* Kyoto, 1985, edited by M. Konuma and K. Takahashi (Research Institute for Fundamental Physics, Kyoto University, Kyoto, 1986), p. 447.

[24]L. D. Landau and E. M. Lifshitz, *Quantum Mechanics,* 3rd ed. (Pergamon, Oxford, 1977), p. 96. We have used their result for the matrix element of a tensor operator and some elementary commutation relations in order to obtain Eq. (2.12).

[25]A. B. Henriques, B. H. Kellett, and R. G. Moorhouse, Phys. Lett. **64B**, 85 (1976); L. H. Chan, *ibid.* **71B**, 422 (1977); see, also, numerous more recent works quoted in Ref. 1.

[26]Yee Jack Ng, James Pantaleone, and S.-H. Henry Tye, Phys. Rev. Lett. **55**, 916 (1985); James Pantaleone, S.-H. Henry Tye, and Yee Jack Ng, Phys. Rev. D **33**, 777 (1986); Moxhay and Rosner (Ref. 21); S. L. Adler and A. C. Davis, Nucl. Phys. **B244**, 469 (1984); S. L. Adler, Prog. Theor. Phys. (Suppl.) **86**, 12 (1986) (Festschrift volume in honor of Y. Nambu).

[27]E. Eichten and F. Feinberg, Phys. Rev. D **23**, 2724 (1981).

[28]T. Sterling, Nucl. Phys. **B141**, 272 (1978); **B148**, 538(E) (1979).

[29]Juliet Lee-Franzini, in *Proceedings of the XXIII International Conference on High Energy Physics* (Ref. 18), p. 669.

[30]R. McClary and N. Byers, Phys. Rev. D **28**, 1692 (1983).

[31]Yu-Ping Kuang and Tung-Mow Yan, Phys. Rev. D **24**, 2874

(1981).
[32]G. Bélanger and Peter Moxhay, Phys. Lett. B **199**, 575 (1987).
[33]Peter Moxhay, Phys. Rev. D **37**, 2557 (1988).
[34]A. Billoire, R. Lacaze, A. Morel, and H. Navelet, Nucl. Phys. **B155**, 493 (1979).
[35]Gary J. Feldman and Frederick J. Gilman, Phys. Rev. D **12**, 2161 (1975); Lowell S. Brown and Robert N. Cahn, *ibid.* **13**, 1195 (1976); Gabriel Karl, Sydney Meshkov, and Jonathan L. Rosner, *ibid.* **13**, 1203 (1976).
[36]Benjamin F. Bayman, lecture notes, University of Minnesota (unpublished). See also, e.g., H. Frauenfelder and R. M. Steffen, in *Alpha, Beta, and Gamma Ray Spectroscopy,* edited by K. Siegbahn (North-Holland, Amsterdam, 1966), p. 997.
[37]S. W. Herb *et al.*, Phys. Rev. Lett. **39**, 252 (1977); W. R. Innes *et al.*, *ibid.* **39**, 1240 (1977); **39**, 1640(E) (1977).
[38]See, e.g., John W. Cooper, in *Proceedings of the XXII International Conference on High Energy Physics,* Leipzig, 1984, edited by A. Meyer and E. Wieczorek (Akademic der Wissenschaften der DDR, Zeuthen, DDR, 1984), Vol. 1, p. 152, and references therein.
[39]E. Rice *et al.*, Phys. Rev. Lett. **48**, 906 (1982); A. Silverman, in *Lepton and Photon Interactions at Higher Energy,* proceedings of the 10th International Symposium, Bonn, 1981, edited by W. Pfeil (Physics Institute, Bonn University, Bonn, Germany, 1981), p. 138.
[40]See, e.g., E. Eichten, Phys. Rev. D **22**, 1819 (1980), and earlier references therein.
[41]See, e.g., Ref. 1 (and references therein) and Ref. 21.
[42]E. Menichetti, in *Proceedings of the First Workshop on Antimatter Physics at Low Energy,* Fermilab, 1986, edited by B. E. Bonner and L. S. Pinsky (Fermilab, Batavia, Illinois, 1986), p. 95

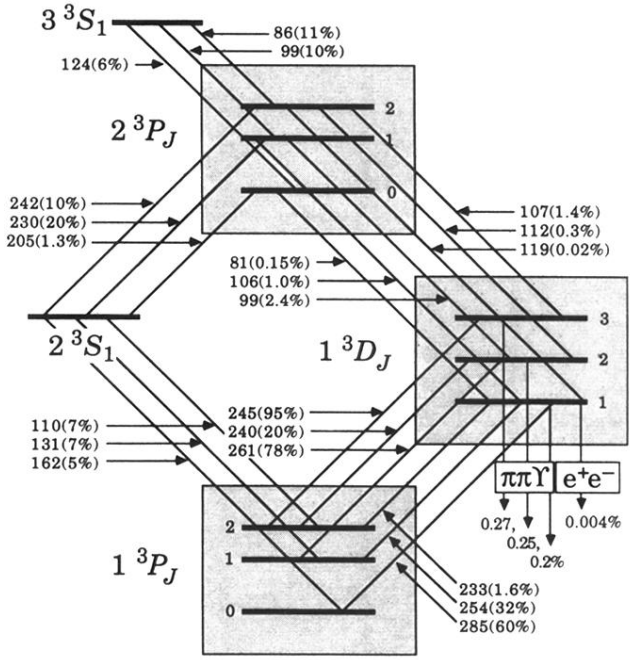

FIG. 4. Branching ratios for radiative transitions in three-photon cascades from $\Upsilon(3\,^3S_1)$ to $\chi_b(1\,^3P_J)$ levels.

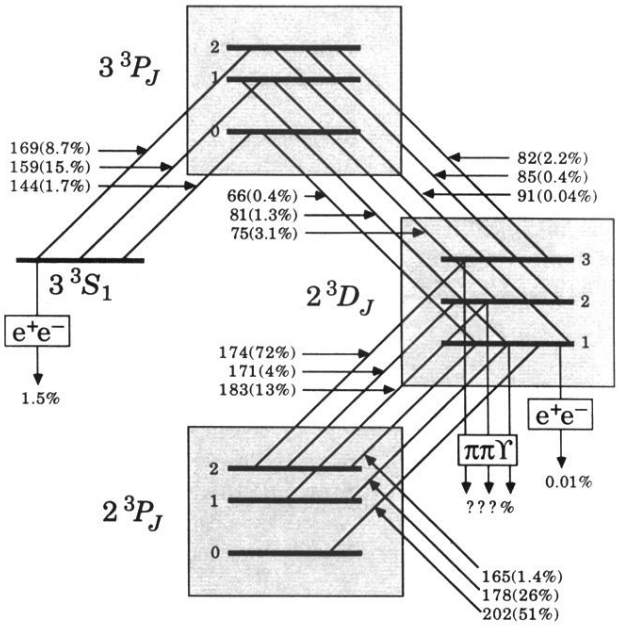

FIG. 9. Branching ratios for radiative transitions from the $3\,^3P\,b\bar{b}$ levels.